Precambrian Research 377 (2022) 106738

Contents lists available at ScienceDirect

Precambrian Research

journal homepage: www.elsevier.com/locate/precamres

Late Neoproterozoic-early Paleozoic tectonic evolution and paleogeographic reconstruction of the eastern Tibetan Plateau: A perspective from detrital zircon U–Pb-Hf isotopic evidence

Zhen-Dong Tian [a,c], Cheng-Biao Leng [a,b,*], Xing-Chun Zhang [a], Feng Tian [a,c], Chun-Kit Lai [d]

[a] State Key Laboratory of Ore Deposit Geochemistry, Institute of Geochemistry, Chinese Academy of Sciences, Guiyang 550081, China
[b] State Key Laboratory of Nuclear Resources and Environment, East China University of Technology, Nanchang 330013, China
[c] University of Chinese Academy of Sciences, Beijing 100049, China
[d] Faculty of Science, Universiti Brunei Darussalam, Gadong BE1410, Brunei

ARTICLE INFO

Keywords:
Detrital zircon
Provenance change
Paleogeographic reconstruction
Yidun Terrane
Eastern Tibetan Plateau

ABSTRACT

The Yidun Terrane, sandwiched between the Qiangtang and Songpan-Ganze terranes, hosts important information on the tectonic evolution of the eastern Tibetan Plateau. However, its tectonic link with adjacent terranes and East Gondwana remains equivocal. Here, we present U-Pb-Hf isotopes of detrital zircons from the upper Neoproterozoic-lower Paleozoic clastic rocks in the Yidun Terrane. The results show that detrital zircons from the Neoproterozoic rocks are mainly of ca. 821 – 890 Ma, 1714 – 1977 Ma, and 2317 – 2520 Ma, with $\varepsilon_{Hf(t)}$ values of each group comparable to coeval magmatic rocks in the nearby South China Block. This suggests that the Yidun Terrane and South China were possibly connected in the late Neoproterozoic, with the latter being the main sedimentary provenance. In contrast, the five Paleozoic samples have markedly different detrital zircon age spectra at ca. 2600 – 2300 Ma, 1100 – 900 Ma, 900 – 740 Ma, and 690 – 480 Ma, which were interpreted to have derived from Pan-African and Grenville-age provinces in the East Gondwana, as well as the South China Block and Songpan-Ganze Terrane. Such a major change on provenance suggests that after prolonged isolation in the Proto-Tethys, the Yidun Terrane began to collide with the East Gondwana in late Ediacaran to early Paleozoic. Integrated with published works, we consider that the Yidun Terrane, along with Songpan-Ganze Terrane and Yangtze Block, was located on the northern margin of East Gondwana during the early Paleozoic.

1. Introduction

The modern Tibetan Plateau was formed by the amalgamation of many allochthonous terranes (e.g., Qiangtang, Lhasa, and Himalaya) (Yin and Harrison, 2000; Metcalfe, 2013, 2021), which were originally rifted from East Gondwana and then progressively drifted northward during the late Paleozoic to Cenozoic periods (Pan et al., 2012). This is accompanied by the opening and closure of the intervening Paleo-Tethys, Meso-Tethys, and Neo-Tethys oceans (Gehrels et al., 2011; Zhu et al., 2011a; Xia et al., 2016; Metcalfe, 2021). Thus, determining the detailed tectonic evolution of each individual terrane is highly important to the tectonic reconstruction of the Tibetan Plateau. Currently, numerous studies were conducted on the origin and tectonic evolution of the Lhasa and Qiangtang terranes (e.g., Zhu et al., 2011a, 2013; Song et al., 2015; Ma et al., 2017, 2018, 2019; Hu et al., 2019; Luo et al., 2020; Wang et al., 2020), yet the tectonic evolution of geological terranes in the eastern Tibetan Plateau is rarely studied.

The Yidun Terrane is one of the representative Precambrian metamorphic terranes in the eastern Tibetan Plateau (Fig. 1a). Due to a large number of Mesozoic porphyry Cu-Mo deposits developed in the terrane, previous studies were mainly focused on Mesozoic regional tectono-metallogenic evolution (e.g., Hou et al., 2001; Li et al., 2011, 2017b; Leng et al., 2012, 2018; Chen et al., 2014a; Peng et al., 2014; Gao et al., 2017; Wu et al., 2017; Tian et al., 2019b; Guo et al., 2020). Pre-Mesozoic tectonic evolution of the terrane remains poorly constrained. Some studies suggested that the Yidun Terrane was rifted from the Yangtze Block during the late Permian Emeishan mantle plume activity (Chang, 2000; Song et al., 2004; Xiao et al., 2004), whereas some argued that it was derived from the eastern Kunlun Terrane by the early Triassic back-arc extension due to the north-dipping Paleo-Tethys subduction (Pullen

* Corresponding author at: State Key Laboratory of Nuclear Resources and Environment, East China University of Technology, Nanchang 330013, China.
E-mail address: lcb8207@163.com (C.-B. Leng).

https://doi.org/10.1016/j.precamres.2022.106738
Received 6 October 2021; Received in revised form 14 May 2022; Accepted 16 May 2022
Available online 30 May 2022

et al., 2008; Ding et al., 2013; Zhang et al., 2014b). Moreover, paleogeographic reconstruction indicates that major geological terranes of the Tibetan Plateau were connected to either the northeastern margin of India Craton (e.g., Qiangtang Terrane) or the northwestern margin of Australia (e.g., Lhasa Terrane) during the Neoproterozoic-early Paleozoic (Zhu et al., 2011a). However, the paleogeographic location of the Yidun Terrane within the Gondwana supercontinent, or whether it was even part of Gondwana remains enigmatic.

Detrital zircons from siliciclastic rocks record a wealth of information about their source regions, and their U-Pb age spectra and Hf isotope composition are useful to unravel the tectonic and paleogeographic affinities (Veevers et al., 2005; Long et al., 2010, 2020; Gehrels, 2012; Burrett et al., 2014; Yao et al., 2014b; Wang et al., 2013a, 2018, 2021; Zhang et al., 2018; Xia et al., 2020). The upper Neoproterozoic to lower Paleozoic sedimentary rocks are good research objects to study any tectonic link between the Yidun Terrane and its surrounding terranes (Fig. 1b), as well as its location relative to Gondwana. However, these sedimentary rocks are poorly understood because of the rugged terrain, high altitude with poor accessibility of the Yidun Terrane.

In this study, we first present detrital zircon in-situ U-Pb age, trace

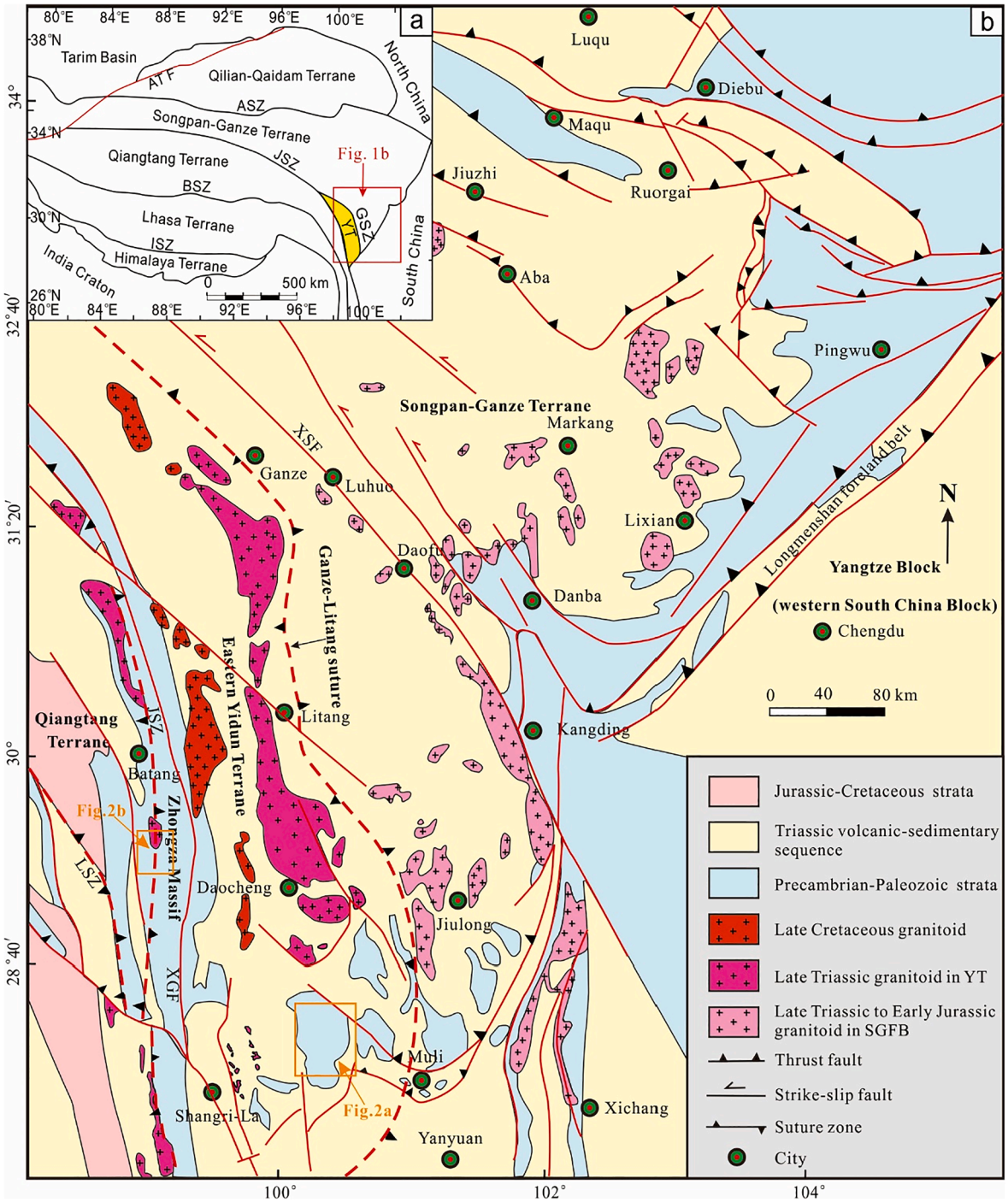

Fig. 1. (a) Sketch map showing the location of Yidun Terrane in the Tibetan Plateau; (b) Simplified geological map of the Yidun Terrane and adjacent regions (after Yan et al., 2008). ASZ: A'nyemaqen Suture Zone; BSZ: Bangong-Nujiang Suture Zone; GSZ: Ganze-Litang Suture Zone; ISZ: Indus-Yarlung Suture Zone; JSZ: Jinshajiang Suture Zone; LSZ: Lancangjiang Suture Zone; ATF: Altyn Tagh Fault; XGF: Xiangcheng-Geza Fault; XSF: Xianshuihe Fault; YT: Yidun Terrane.

element, and Lu-Hf isotope data for the upper Neoproterozoic to lower Paleozoic sedimentary rocks in the Yidun Terrane. We aim to (i) identify the sediments provenance of these rocks, (ii) clarify the tectonic affinity of the Yidun Terrane, and (iii) reveal any tectonic link between the Yidun Terrane and Gondwana.

2. Regional geology

Tectonically, the Yidun Terrane is separated from the Qiangtang Terrane to the west by the Jinshajiang Suture Zone, and from the Songpan-Ganze Terrane and South China Block to the east by the Ganze-

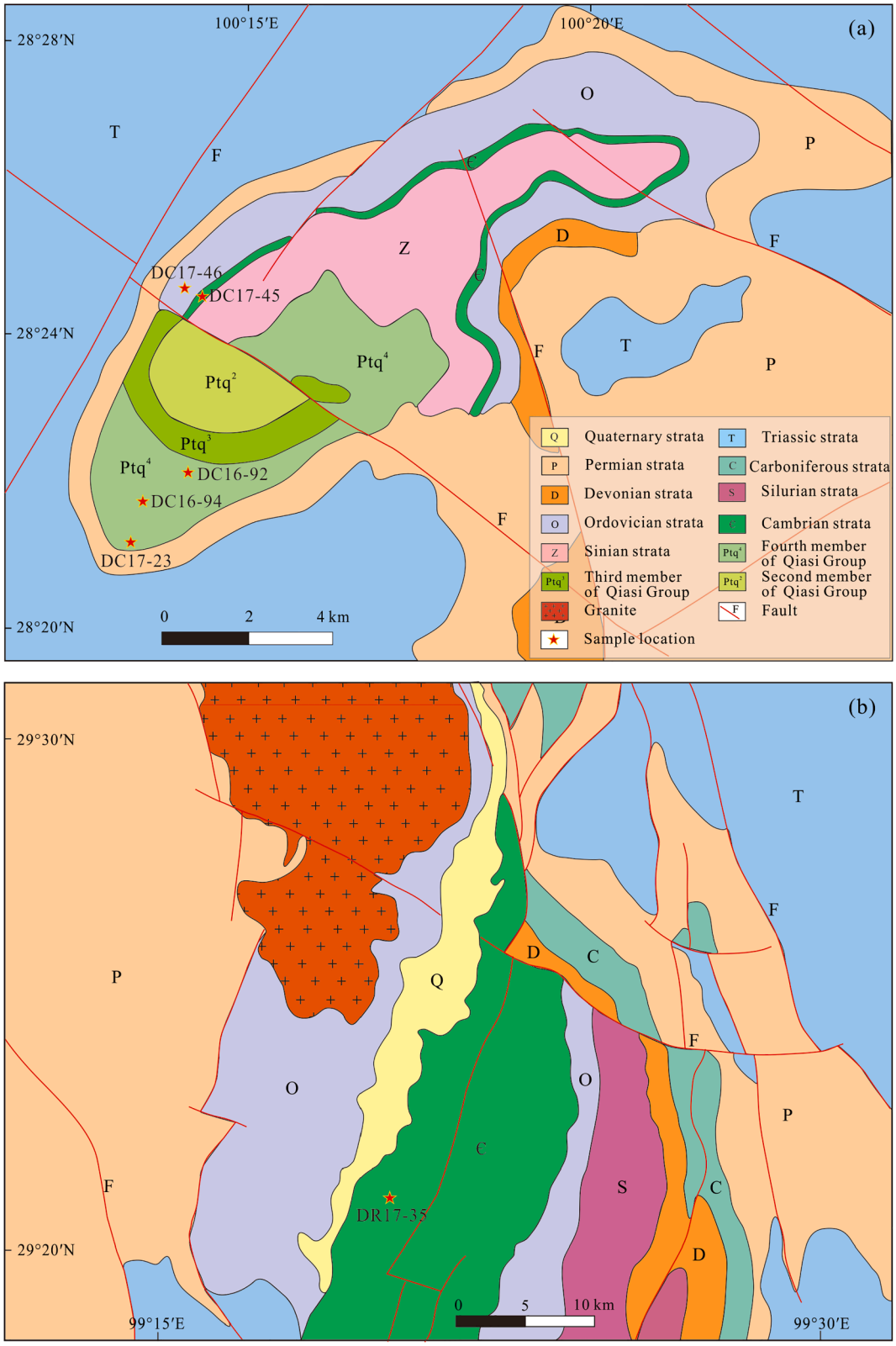

Fig. 2. Geological maps of the Kasi (a) and Zhongza (b) areas in the Yidun Terrane, showing sampling locations.

Litang Suture Zone. Geological setting of these four terranes/blocks and two sutures are summarized as below:

2.1. The Yidun Terrane

The Yidun Terrane is composed of Precambrian crystalline basement and overlying Paleozoic to Triassic sedimentary rocks. It can be geologically divided into two units, the western Yidun Terrane and eastern Yidun Terrane, by the NNW-trending Xiangcheng-Geza fault (Fig. 1b). The western Yidun Terrane (also known as the Zhongza massif) is mainly composed of Paleozoic shallow to deep marine carbonates and clastic rocks with volcanic interbeds, whereas the eastern Yidun Terrane is dominated by Triassic volcanic-sedimentary successions with minor Precambrian to early Paleozoic basement rocks (Tian et al., 2019a).

The oldest strata in the Yidun Terrane is the Qiasi Group, which is only exposed in the southern segment of eastern Yidun Terrane (Fig. 2a), and were long considered to be Precambrian basement of the Yidun Terrane (BGMRSP, 1991). The Qiasi Group has undergone different degrees of metamorphism and deformation, and can be divided into four members (Du, 1986; BGMRSP, 1991): (from the bottom to top) (i) schist and leptynite; (ii) schist with minor felsic volcanic and marble interbeds; (iii) albite leptynite and sandstone, with minor schist (Tian, 2020); (iv) sandstone with local schist interbeds. The field contact relations between the different members are obscured by dense vegetation and slope sediments. The Qiasi Group is in fault contact with the Sinian strata (Tian, 2020), which is in turn overlain by the lower Paleozoic sequences. The Cambrian strata are sandwiched between the Sinian and lower Ordovician strata (Fig. 2a), and are dominated by shallow marine carbonates with minor sandstone interbeds. Due to the lack of index fossils or radiometric age data, the age of the strata is loosely constrained (BGMRSP, 1991). The Ordovician strata overlie conformably on the Cambrian strata, and are composed mainly of sandstone, siltstone, and slate. These lower Paleozoic strata are overlain by Devonian carbonate and mica-schist, as well as Permian volcanic-sedimentary sequence (Fig. 2a).

Lower Paleozoic strata are widely exposed in the western Yidun Terrane (Fig. 2b). The Cambrian strata consist mainly of shallow marine carbonate, sandstone, slate, and schist. Fossils in the strata include trilobite (e.g., *Calvine* sp., *Haniwa* sp., *Saukiidae*) and brachiopods (e.g., *Finkelnburgia* sp., *Palaeostrophia* sp., and *Apheoorthis* sp.) (Zheng et al., 1984). The Ordovician strata overlie conformably on the Cambrian strata, and are composed mainly of marine carbonate with minor slate interlayer. Fossils in the strata include graptolite (e.g., *Callograptus* sp.), trilobite (e.g., *Asaphidae* and *Leiostegiidae*), and brachiopods (e.g., *Leptellina* sp., and *Aporthophyla* sp.). The Silurian strata overlie conformably on the Ordovician strata and are dominated by marine carbonate rocks. These Paleozoic sedimentary rocks in the western Yidun Terrane have undergone greenschist- to lower amphibolite-facies metamorphism (Reid et al., 2005a, 2005b).

Magmatic rocks in the Yidun Terrane are mainly formed in the late Triassic (ca. 230 – 206 Ma) and late Cretaceous (ca. 88 – 80 Ma) (Tian et al., 2019a). The late Triassic magmatic rocks consist of both intrusive (e.g., diorite, monzonite, granodiorite, granite) and extrusive (e.g., basalt, andesite, dacite, and rhyolite) rocks, which were interpreted as products of the westward subduction of the Ganze-Litang Paleo-Tethys Ocean at late Triassic (Wang et al., 2011a; Huang et al., 2012; Leng et al., 2014; Wu et al., 2017). In contrast, the Cretaceous igneous rocks are predominantly plutonic, and include (biotite) granite, monzogranite, and granitic porphyry. They were suggested to have formed in an intraplate extensional setting (Wang et al., 2014a; Li et al., 2017b; Yang et al., 2017).

2.2. The Ganze-Litang Suture Zone

This suture zone is about 1000 km long and 5 – 70 km wide (Hou et al., 2003; Yang et al., 2012), and forms the boundary between the Yidun and Songpan-Ganze terranes. To the north, the suture zone merges with the Jinshajiang Suture Zone, while to the south it passed into a transitional zone between the South China Block and Qiangtang Terrane (Jackson et al., 2020). Ophiolites, exposed sporadically in the suture, include metamorphosed peridotite, cumulate gabbro, diabase, mid-ocean-ridge basalt, and Devonian to Triassic radiolarian cherts (Hou et al., 2003; Li et al., 2017a). Previous plagioclase ^{40}Ar-^{39}Ar and zircon U-Pb dating constrained the ophiolite formation to 292 – 231 Ma (Qu and Hou, 2002; Yan et al., 2005), indicating an early Permian to middle Triassic development of the Ganze-Litang ocean.

2.3. The South China Block

The South China Block comprises the Yangtze and Cathaysia blocks, which were welded along the Jiangnan Orogen in the middle Neoproterozoic (~830 Ma) (Zhao et al., 2011). The Yangtze Block comprises Archean (e.g., Kongling Complex: ~3300 – 2900 Ma, Gao et al., 2011; Yudongzi Complexe: ~2700 – 2500 Ma, Chen et al., 2019; and Douling Complex: ~2500 Ma, Hu et al., 2013) and Paleoproterozoic (e.g., Phan Si Pan gneiss: ~2280 – 2190 Ma, Wang et al., 2016; Quanqitang granite: ~1850 Ma, Peng et al., 2012) crystalline basement, which was unconformably overlain by Neoproterozoic to middle Triassic marine sedimentary rocks. Neoproterozoic (ca. 870 – 730 Ma) granite, diorite, gabbro, TTG genesis, and their volcanic equivalence are widespread in the western and northern Yangtze Block (Zhou et al., 2006; Wang et al., 2008; Zhao et al., 2008b, 2010a, 2018; Zhu et al., 2019a). These magmatic rocks were interpreted to have formed by subduction-related (Zhou et al., 2002) or mantle plume-related magmatism (Li et al., 2002, 2003).

Unlike the Yangtze Block, no Archean rocks have been found in the Cathaysia Block. The oldest basement rocks in the Cathaysia Block are Paleoproterozoic (~1900 – 1800 Ma) granitoids and supracrustal rocks, as represented by the Badu Complex (Yu et al., 2009). These basement rocks are unconformably overlain by Neoproterozoic to Cretaceous sedimentary sequences. Magmatism in the Cathaysia Block mainly occurred during the Jinningian (850 – 770 Ma), Kwangsian (430 – 400 Ma), Indosinian (245 – 200 Ma), and Yanshanian (170 – 120 Ma) orogenic events (Wang et al., 2010; Duan et al., 2012).

In addition to the Yangtze and Cathaysia blocks interior, middle to late Neoproterozoic igneous rocks are also widely exposed in the Jiangnan Orogen. Previous studies suggested that these rocks were produced by partial melting of mafic rocks in the lower crust or recycled heterogeneous supracrustal materials (Wang et al., 2006, 2011b; Zheng et al., 2007; Zhao et al., 2013a; Yao et al., 2014a; Lv et al., 2021).

2.4. The Songpan-Ganze Terrane

The terrane is triangular-shaped (outcrop size: >200,000 km^2) and located at the junction of the Yidun, Yangtze, Qiangtang, North China, and Kunlun terranes/blocks (Chang, 2000; Burchfiel and Chen, 2012). Sedimentary rocks in the terrane are almost exclusively middle to upper Triassic flysh, with a thickness of 5 – 15 km (Nie et al., 1994; Enkelmann et al., 2007). Provenance studies reveal that most of the detritus were sourced from the neighboring North China, Yangtze, and Kunlun terrane/blocks and Qinlin-Dabie Orogen (Nie et al., 1994; Bruguier et al., 1997; She et al., 2006; Weislogel et al., 2006; Enkelmann et al., 2007). Pre-Triassic rocks are exposed sporadically in a NE-trending belt within/close to the Longmenshan Thrust Fault, which separates the Songpan-Ganze Terrane from the Yangtze Block (Burchfiel et al., 1995; Burchfiel and Chen, 2012). These pre-Mesozoic strata are interpreted to be allochthonous, and were dismembered from the western part of Yangtze Block (Burchfiel and Chen, 2012). Hence, the nature of basement rocks (oceanic or continental) below the Triassic sediments is still unclear (Burchfiel and Chen, 2012; Nie et al., 1994). Granitoids in the Songpan-Ganze Terrane were mainly formed from the late Triassic to

early Cretaceous, and are interpreted to be generated by partial melting of the thickened crust during a regional shortening event (Roger et al., 2004), or by lithospheric delamination (Zhang et al., 2007). In addition, some Neoproterozoic igneous rocks, such as the Xuelongbao adakitic complex (748 ± 7 Ma; Zhou et al., 2006), Gongcai magmatic granites (822 ± 14 Ma; Zhou et al., 2002), and Gezong granite (864 ± 8 Ma; Zhou et al., 2002), are also documented.

2.5. The Qiangtang Terrane

The terrane is bounded by the Jinshajiang Suture Zone to the north and the Bangong-Nujiang Suture Zone to the south, and can be divided into the North Qiangtang and South Qiangtang terranes by the Triassic Shuanghu suture. The Qiangtang Terrane consists of Proterozoic to early Paleozoic metamorphic basement (e.g., Gemuri Group) intruded by Ordovician granitoids (ca. 470 Ma) (Yin and Harrison, 2000; Gehrels et al., 2011; Zhu et al., 2013). These basement rocks are overlain by Carboniferous to Triassic marine strata and mafic rocks: the upper Carboniferous sequence contains abundant glacial-marine diamictites and basalt interlayers (Zhu et al., 2013), and the intruding 302 – 284 Ma mafic dykes (Zhai et al., 2009). Apart from the Paleozoic magmatism, extensive early Jurassic-middle Cretaceous (183 – 101 Ma) arc-type magmatic rocks are developed (Zhang et al., 2012c. and references therein). In addition, some high-pressure metamorphic rocks, including blueschist, phengite-schist, eclogite, and matabasite, were documented in the central Qiangtang Terrane (Zhang et al., 2012c; Zhu et al., 2013).

2.6. The Jinshajiang Suture Zone

The suture is located between the western Yidun and Qiangtang terranes, and contains remnants of the Paleo-Tethyan Jinshajiang Ocean (Metcalfe, 2013). It extends southward to connect with the Ailaoshan Suture Zone. Previous studies suggested that the Jinshajiang and Ailaoshan suture zones are contiguous and represent the same ocean basin (Wang et al., 2000; Jian et al., 2009). Ophiolitic mélanges in the suture zone are mainly composed of dismembered peridotite, cumulate gabbro, pillow lava, and limestone and radiolarian chert. Zircon U-Pb dating shows that the cumulate gabbro in the suture zone was formed at 343.4 ± 2.7 Ma (Jian et al., 2009), and the plagiogranite was formed at 340 ± 3 Ma and 294 ± 3 Ma (Wang et al., 2000). However, the cumulate gabbro and plagiogranite in the Ailaoshan Suture Zone are older (383 – 362 Ma; Wang et al., 2000; Jian et al., 2009; Lai et al., 2014a). This suggests that the Jinshajiang-Ailaoshan ocean basins were formed before the middle Devonian (~383 Ma). Consumption of the Paleo-Tethyan Jinshajiang Ocean was resulted from its westward subduction beneath the Qiangtang Terrane, which generated numerous late Permian to early Triassic (ca. 250 – 230 Ma) subduction-/collision-related magmatic units (Zhu et al., 2011b; Zi et al., 2012a, 2012b; Lai et al., 2014b).

3. Sampling and analytical methods

3.1. Sampling

Based on detailed field geological investigations, six representative sedimentary samples were collected from the Yidun Terrane. Among these samples, three (DC16-92, DC16-94, DC17-23) were collected from the Qiasi Group (4th member), and two (DC17-45, DC17-46) from the previously-assigned Cambrian and Ordovician strata, respectively, at Kasi Village (Daocheng County) in the eastern Yidun Terrane. One sample (DR17-35) was taken from the well-defined lower Cambrian strata at Zhongza Town (Derong County) in the western Yidun Terrane. All the samples have similar mineral assemblages, consisting mainly of quartz, plagioclase, K-feldspar, mica, and minor chlorite. The detailed rock type, mineral content, and GPS location of each sample are summarized in Table 1. Representative field photos and thin-section micrographs of these rocks are shown in Fig. 3.

3.2. LA-ICP-MS U-Pb dating and trace element analyses

Zircon grains were separated from the samples using conventional magnetic and heavy liquid techniques, and were then hand-picked under a binocular microscope. Over 200 zircon grains for each sample were randomly selected, mounted in epoxy resin on a 2 cm diameter disk, then polished to half of their thickness for analyses. Prior to in-situ U-Pb isotope and trace element analyses, all zircons were examined by transmitted/reflected optical microscopy, and cathodoluminescence (CL) imaging to reveal their external and internal structure. CL images were undertaken on a JSM-7088F type thermal field scanning electron microscope attached with a Gatan Mono CL4 detector at Institute of Geochemistry, Chinese Academy of Sciences (IGCAS). Detrital zircons, without obvious cracks or inclusions, were randomly selected for U-Pb isotopic and trace element analyses at IGCAS. Zircon U-Pb dating and trace element analyses were synchronously conducted by an Agilent 7900 Inductively Coupled Plasma Mass Spectrometer (ICP-MS) coupled to a GeoLas Pro 193 nm ArF excimer laser ablation system. Analyses were performed with a spot diameter of 32 μm and a repetition rate of 5 Hz. Helium was applied as a carrier gas which is mixed with Argon via a T-connector before entering the ICP-MS. Each analysis includes circa 20 s background signal followed by 40 s data acquisition from the sample. Harvard zircon 91,500 was used as the external standard to correct instrumental mass bias, depth-dependent elemental, and isotopic fractionation. It was analyzed twice before and after ten analyses. Zircon Plešovice and Qinghu were analyzed as quality controls and analyzed

Table 1
Location, lithologies, and stratigraphic information of the samples analyzed.

Sample	GPS coordinates	Stratigraphic information	Lithology	Mineral composition	Maximum age (Ma)
Eastern Yidun Terrane					
DC16-92	N28°22′7.8″ E100°14′17.5″	Qiasi Group (4th member)	Fine sandstone	Quartz (70%), K-feldspar (10–15%), plagioclase (5–10%), mica (<5%), and minor heavy minerals	510 ± 8.6 Ma
DC16-94	N28°21′04.4″ E100°13′16.5″	Qiasi Group (4th member)	Greywacke	Quartz (60–65%), K-feldspar (15–20%), plagioclase (10–15%), and minor heavy minerals	456 ± 6.6 Ma
DC17-23	N28°21′0.30″ E100°13′25.20″	Qiasi Group (4th member)	Medium-/fine-grained feldspathic quartz sandstone	Quartz (65–70%), K-feldspar (10–15%), plagioclase (5–10%), mica (<5%), and minor heavy minerals	515 ± 4.8 Ma
DC17-45	N28°24′28.22″ E100°14′37.07″	Cambrian (?)	Medium-grained quartz arenite	Quartz (85–90%), feldspar (<5%), mica (<5%), and minor heavy minerals	637 ± 5 Ma
DC17-46	N28°24′30.60″ E100°14′30.50″	Ordovician	Fine feldspathic quartz sandstone	Quartz (65–70%), plagioclase (10–15%), K-feldspar (5–10%), mica (<5%), and minor heavy minerals	525 ± 5 Ma
Western Yidun terrane					
DR17-35	N29°20′59.08″ E99°20′24.73″	Lower Cambrian	Fine-grained sandstone	Quartz (70–75%), plagioclase (5–10%), mica (10–15%), and minor heavy minerals	532 ± 7.9 Ma

Note: the maximum depositional age of each sample was constrained by the youngest age of detrital zircon in this study.

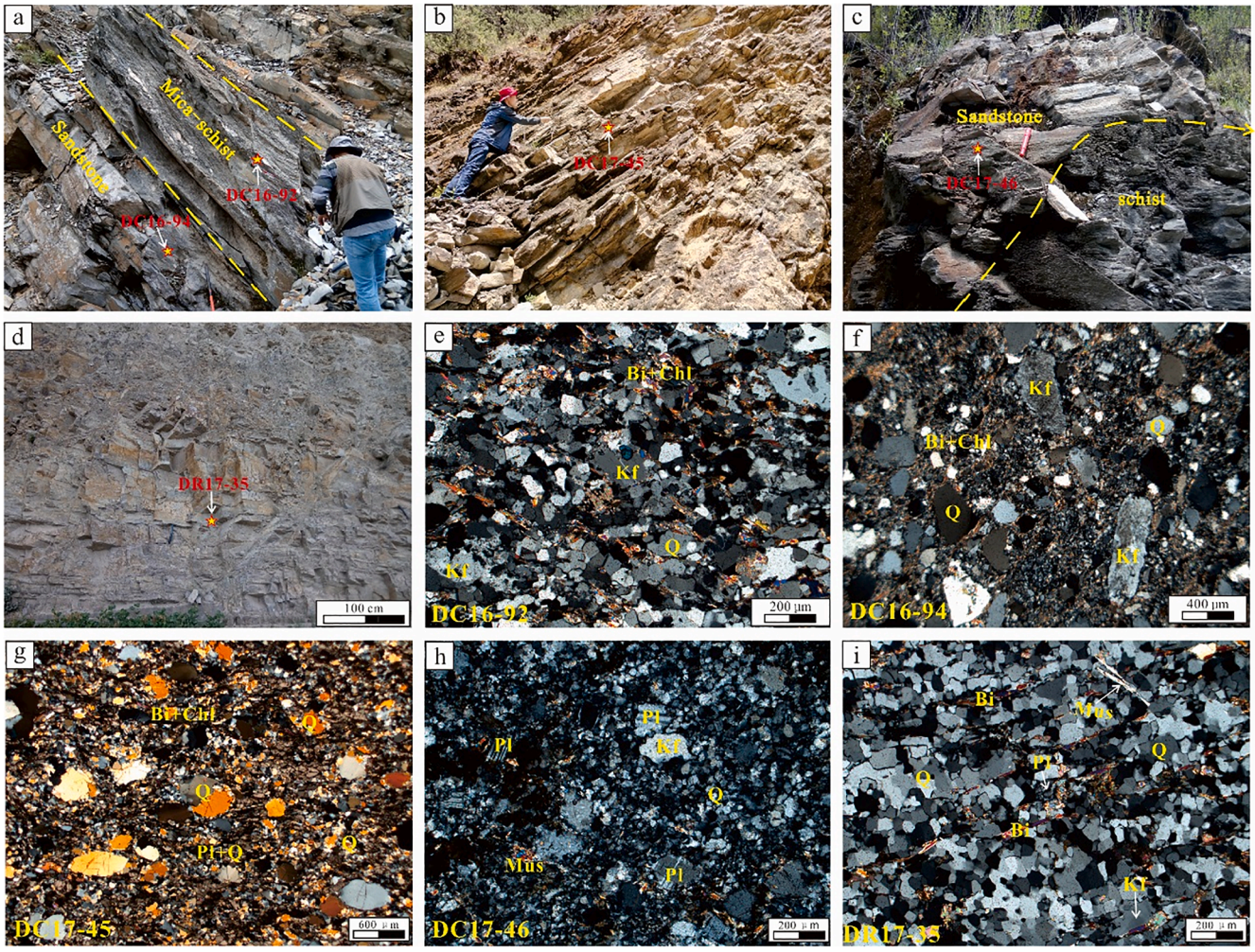

Fig. 3. Representative field photos (a-d) and thin-section photomicrographs (e-i) of the samples used for zircon U-Pb dating. Mineral abbreviations: Bi-biotite, Chl-Chlorite, Kf-potassium feldspar, Mus-Muscovite, Pl-Plagioclase, Q-Quartz.

once before and after ten analyses. NIST SRM610 glass was used as the external standard to normalize U, Th, Pb concentrations of the unknowns, whilst zircon ^{29}Si concentration was used for internal standardization. Trace element compositions of zircons were calibrated against multiple reference materials (BCR-1G and BCR-2G) combined with the internal standardization (Liu et al., 2010). The analytical results of standard zircons Plešovice and Qinghu yielded respective weighted mean $^{206}Pb/^{238}U$ ages of 337 ± 2 Ma and 160 ± 2 Ma, consistent with their corresponding recommended values o 337.13 ± 0.37 Ma (Sláma et al., 2008) and 159.5 ± 0.2 Ma (Li et al., 2013b) within errors. Off-line selection and integration of background and analytic signals, and time-drift correction and quantitative calibration for U-Pb dating and trace element analyses were performed with the ICPMSDataCal program (Liu et al., 2008b, 2010). The age calculations and the concordia plotting were made using Isoplot/Ex_ver4.15 (Ludwig, 2003). Individual analyses in the data table and concordia plots are present at 1σ and age uncertainty is quoted at the 95% confidence level.

3.3. In-situ Hf isotope analysis

After LA-ICP-MS zircon U-Pb dating, Lu-Hf isotope analyses were carried out using a Neptune Plus multi-collector inductively coupled plasma mass spectrometer (MC-ICP-MS) coupled with a Geolas HD excimer ArF laser ablation system (Coherent, Göttingen, Germany) at the Wuhan Sample Solution Analytical Technology Co. Ltd. (China). In situ Hf isotope analyses were conducted at/near the U-Pb dated domain. The laser ablation beam was 44 μm in diameter and the analysis used 8 Hz laser repetition rate and 7 J/cm^2 laser energy. Each measurement was made up of 20 s background signal acquisition followed by 50 s ablation signal acquisition, resulting in 20 – 40 μm-deep pits. Helium was used as a carrier gas to transport the ablated aerosol, and argon as a make-up gas to mix with the carrier gas. Standard zircons 91,500 and GJ-1 were used to monitor the accuracy of interference correction during the analyses. Zircon 91,500 and GJ-1 yielded weighted average $^{176}Hf/^{177}Hf$ ratios of 0.282310 ± 0.000010 and 0.282009 ± 0.000007, respectively, consistent (within error) with their respective recommended values of 0.282311 ± 0.000005 (Yuan et al., 2008) and 0.282013 ± 0.000004 (Yuan et al., 2008). Detailed operating conditions and analytical procedures were similar to those described by Hu et al. (2012). Off-line selection and integration of analyte signals and mass bias calibrations were performed with ICPMSDataCal (Liu et al., 2010). A decay constant of 1.865 × 10^{-11} year^{-1} for ^{176}Lu was adopted (Scherer et al., 2001), and the initial Hf isotope ratios were calculated relative to the chondritic reservoir with a $^{176}Hf/^{177}Hf$ ratio of 0.282772 and $^{176}Lu/^{177}Hf$ of 0.0332 (Blichert-Toft and Albarède, 1997). The depleted mantle line is defined by the present-day $^{176}Hf/^{177}Hf$ and $^{176}Lu/^{177}Hf$ ratios of 0.28325 and 0.0384, respectively (Griffin et al., 2004). Two-stage Hf model ages (T_{DM2}) were calculated for the source rocks of the magma by assuming a mean $^{176}Lu/^{177}Hf$ value of 0.015 for the average continental crust (Griffin et al., 2000).

4. Results

4.1. Zircon morphology and origin

Zircons from the investigated samples are colorless to light pink and exhibit a significant difference in size and morphology. They are 50 – 200 μm long and 40 – 90 μm wide, with length to width ratios of 1:1 to 3:1 (Fig. 4). Typically, these zircon grains are (sub)rounded, indicating prolonged and/or possibly multicycle transport (Fedo et al., 2003). Some zircon grains are subhedral-euhedral prismatic, suggestive of a proximal source.

Zircon CL imaging and Th/U ratios define three zircon types. Most zircons display varying intensity (strong to weak) of oscillatory zoning and high Th/U ratios (typically > 0.2) (Figs. 4 and 5), indicative of an igneous origin (Hanchar and Rudnick, 1995; Corfu et al., 2003). A few zircon grains show dark or homogeneous internal structure (Fig. 4), with low Th/U ratios of < 0.09 (Fig. 5), consistent with a metamorphic origin. In addition, a few zircon grains show complex internal structures with oscillatory-zoned or homogeneous cores overgrown by unzoned rims (Fig. 4).

4.2. Detrital zircons U-Pb age and Hf isotope compositions

A total of 475 zircon grains from six representative sedimentary samples were analyzed, in which 459 grains yielded < 10% discordance and were considered suitable for provenance analysis. The zircon U-Pb dating and Hf isotope analysis results are given in supplementary Table S1 and Table S2, respectively, and presented in Fig. 6 and Fig. 7. $^{207}Pb/^{206}Pb$ and $^{206}Pb/^{238}U$ ages are used for zircon grains older and younger than 1000 Ma, respectively. All analyses are plotted on concordia diagrams, while only those within 90% concordance are included in the frequency plots and discussed below.

4.2.1. Qiasi Group (4th member) (DC16-92, DC16-94, and DC17-23)

The three samples have similar age ranges and spectra. A total of 235 zircon grains were dated, yielding 227 concordant ages (<10% discordance) from 3349 to 456 Ma. This indicates either input from multiple source regions or from source rocks with diverse ages (Fedo et al., 2003). Four age populations were identified: 2331 – 2595 Ma (n = 36 (15.9%); peak ~ 2467 Ma), 900 – 1095 Ma (n = 71 (31.3%); peak ~ 967 Ma), 754 – 864 Ma (n = 24 (10.6%); peak ~ 816 Ma), and 507 – 625 Ma (n = 25 (11.0%); peak ~ 579 Ma) (supplementary Table S1 and Figure S1). Furthermore, forty-nine (21.6%) zircons yield $^{207}Pb/^{206}Pb$ ages of 1100 – 2244 Ma, and eleven (4.8%) detrital zircons have Archean $^{207}Pb/^{206}Pb$ ages of 2648 – 3349 Ma. The youngest zircon has a concordant $^{206}Pb/^{238}U$ age of 456 ± 6.6 Ma, representing the maximum depositional age of the strata.

Hafnium isotope analyses were made on 176 zircons from these three samples. The 2331 – 2595 Ma zircons have $^{176}Hf/^{177}Hf$ ratios = 0.280796 – 0.281569, $\varepsilon_{Hf(t)}$ = -18.7 to + 12.2, and two-stage model ages

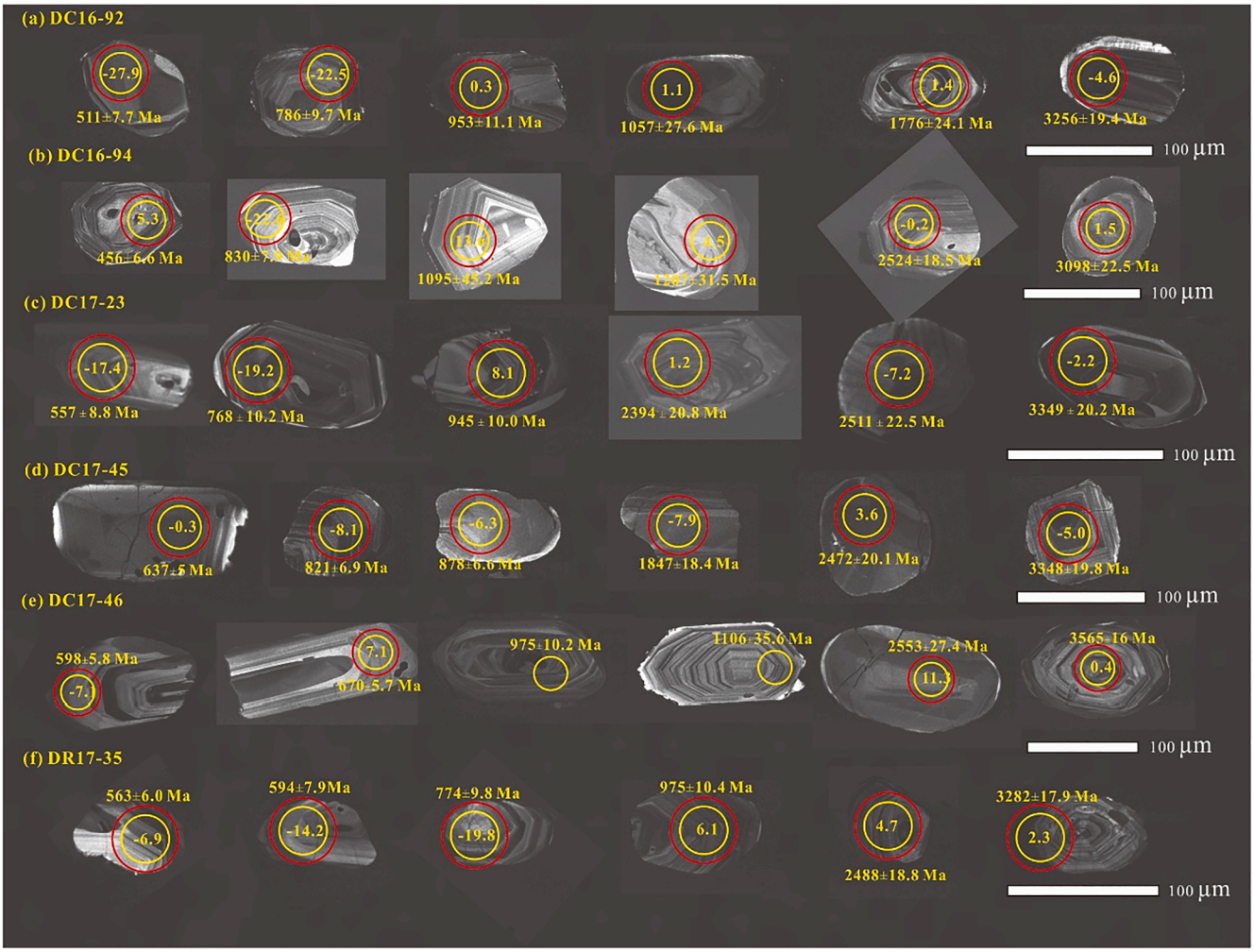

Fig. 4. Representative cathodoluminescence (CL) images of detrital zircon grains from six samples in the Yidun Terrane. The yellow and red circles represent the U-Pb and Hf isotopic analyzed spots, respectively. (For interpretation of the references to colour in this figure legend, the reader is referred to the web version of this article.)

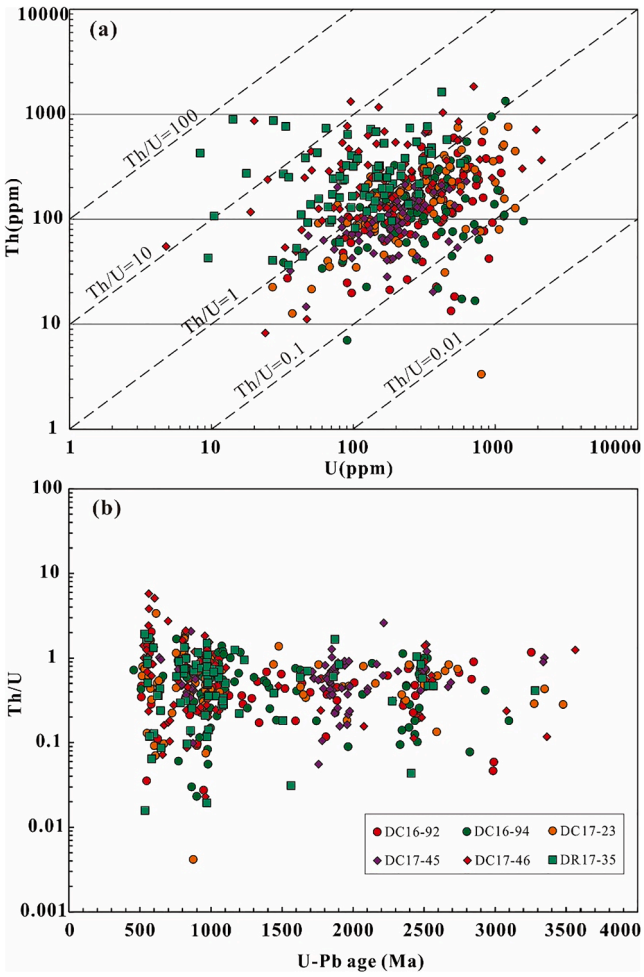

Fig. 5. Plots of U vs. Th (a) and U-Pb age vs. Th/U (b) for detrital zircon in our samples.

(T_{DM2}) of 2226 – 4010 Ma (supplementary Table S2, Fig. 7a). The 900 – 1095 Ma zircons have $^{176}Hf/^{177}Hf = 0.281159 – 0.282541$, $\varepsilon_{Hf(t)} = -36.2$ to + 13.6, and T_{DM2} = 1058 – 4044 Ma (supplementary Table S2, Fig. 7a). The 754 – 864 Ma zircons have $\varepsilon_{Hf(t)}$ = –22.7 to + 10.4 and corresponding T_{DM2} = 1052 – 3118 Ma (supplementary Table S2, Fig. 7a). The 507 – 625 Ma zircon have $\varepsilon_{Hf(t)}$ = -27.9 to + 13.5 and T_{DM2} = 615 – 3204 Ma.

4.2.2. Cambrian strata (DC17-45 and DR17-35)

Sample DC17-45 from the eastern Yidun Terrane has a distinctively different zircon age spectrum and ranges from the well-defined lower Cambrian strata (e.g., DR17-35) in the western Yidun Terrane. For sample DC17-45, a total of 80 detrital zircons (yielding 79 concordant ages) were dated to be 637 Ma to 3348 Ma. The detrital zircon age pattern of this sample is distinctly different from other samples mentioned above, as characterized by two major age groups of 821 – 890 Ma (n = 16; peak ~ 869 Ma) and 1714 – 1977 Ma (n = 39; peak ~ 1843 Ma), and a minor age group of 2317 – 2520 Ma (n = 9; peak ~ 2496 Ma) (Fig. 6h). Importantly, late Mesoproterozoic-early Neoproterozoic and early Paleozoic detrital zircons are absent in this sample, but they are abundant in sample DR17-35 (see below) and other samples from the Qiasi Group (4th member). The oldest and youngest zircon in this sample is 3348 ± 19.8 Ma and 637 ± 5 Ma, respectively. A total of 59 concordant zircons were analyzed for their Hf isotope compositions. The 2317 – 2520 Ma zircons have negative to positive $\varepsilon_{Hf(t)}$ values (-17.3 to 3.7), which correspond to T_{DM2} = 2757 – 4061 Ma (Fig. 7b). Except for one analysis, twenty-six zircons (1714 – 1977 Ma) have negative $\varepsilon_{Hf(t)}$ values (-10.2 to −0.4) and T_{DM2} ages ranging from 2455 to 3093 Ma. The 821 – 890 Ma zircons all have negative $\varepsilon_{Hf(t)}$ (-26.6 to −4.2), corresponding to the T_{DM2} of 2011 – 3392 Ma.

Eighty zircon grains from sample DR17-35 were U-Pb dated, among which 77 are concordant and fall on/near the concordia. The age population is pretty similar to that of samples from the Qiasi Group (4th member) (i.e., DC16-92, DC16-94, and DC17-23) in the eastern Yidun Terrane. It is characterized by a predominant late Mesoproterozoic-early Neoproterozoic cluster (910 – 1087 Ma; n = 28) with an obvious peak at ~ 974 Ma, and two subordinate clusters of 774 – 894 Ma (n = 12, peak ~ 818 Ma) and 532 – 598 Ma (n = 11, peak ~ 554 Ma) (Fig. 6l). Moreover, some zircon grains are clustered around 2276 – 2567 Ma (n = 7). The oldest and youngest zircon in the sample are 3283 ± 17.9 Ma and 532 ± 7.9 Ma, respectively, with the latter defining the maximum depositional age. Sixty dated concordant zircons from this sample were analyzed for Hf isotopes. The major zircon population at 910 – 1087 Ma have varying $\varepsilon_{Hf(t)}$ values (-14.9 to + 10.3) and T_{DM2} = 1225 – 2825 Ma (Fig. 7a). The 774 – 894 Ma zircons have $\varepsilon_{Hf(t)}$ = -25.2 to + 6.3 and T_{DM2} = 1284 – 3272 Ma, whilst the 532 – 598 Ma zircons have $\varepsilon_{Hf(t)}$ = -14.8 to + 6.3 and wide T_{DM2} range of 1284 – 2433 Ma. The 2276 – 2567 Ma zircons have $\varepsilon_{Hf(t)}$ = -28.4 to + 4.7 and T_{DM2} = 2704 – 4536 Ma.

4.2.3. Ordovician strata (DC17-46)

A total of 80 zircon grains were analyzed, yielding 76 concordant ages (525 – 3565 Ma) that fall into four clusters: 525 – 598 Ma (n = 16 (21%); peak ~ 560 Ma), 801 – 886 Ma (n = 10 (13%); peak ~ 824 Ma), 922 – 1106 Ma (n = 25 (33%); peak ~ 974 Ma), and 2428 – 2558 Ma (n = 7 (9.2%); peak ~ 2502 Ma) (Fig. 6j). In addition, eleven zircon grains have U-Pb ages of 603 – 709 Ma, and Proterozoic (1476 – 2076 Ma, n = 4) and Archean (3081 – 3565 Ma, n = 3) zircons were also identified. The youngest zircon age (525 ± 5 Ma) defines the upper limit of depositional age.

A total of 53 concordant zircons from this sample were Hf isotope analyzed. The 922 – 1106 Ma zircons have mostly negative $\varepsilon_{Hf(t)}$ values (-17.3 to −1.3), although few zircons have positive $\varepsilon_{Hf(t)}$ values (+0.5 to + 10.6) (Fig. 7a). The corresponding T_{DM2} of the 922 – 1106 Ma zircons are 1161 – 2897 Ma. The 801 – 886 Ma zircons have $\varepsilon_{Hf(t)}$ = -27.5 to + 4.1 and a wide T_{DM2} range (1504 – 3414 Ma). All the 525 – 598 Ma zircons have negative $\varepsilon_{Hf(t)}$ values (-28.1 to −1.2) and wide T_{DM2} ranges (1578 – 3253 Ma), indicating that their parent magmas were produced by reworking of the Archean-Paleoproterozoic continental crust. Besides, four 2428 – 2558 Ma zircons have $\varepsilon_{Hf(t)}$ = -1.9 to + 11.3 and T_{DM2} = 2348 – 3103 Ma.

4.3. Detrital zircon trace element compositions

Typically, zircons with magmatic origin have Th/U ratios higher than 0.1, HREE-enriched and LREE-depleted patterns, and marked positive Ce but negative Eu anomalies; whilst metamorphic zircons are generally depleted in HREEs, and have low Th/U ratios (<0.1) and flat REE patterns without negative Eu anomaly (Hoskin and Ireland, 2000; Hoskin and Schaltegger, 2003). In this study, most of the zircons analyzed display clear negative Eu anomalies, positive Ce anomalies, and distinct HREE-enriched patterns (Fig. 8), consistent with the magmatic origin. In addition to distinguishing its origin, trace elements (e.g., U, Yb, Hf, Y) of zircon can also fingerprint the source rock types (Belousova et al., 2002). Most detrital zircons in this study have relatively high U (100 – 1846 ppm), but low Y (35.9 – 4718 ppm), Yb (8.31 – 1445 ppm), and Hf (5106 – 18379 ppm) concentrations (supplementary Table S1). In the U/Yb versus Hf and U/Yb versus Y discrimination diagrams (Fig. 9a and b), almost all detrital zircons analyzed fall inside the continental zircon field, precluding an oceanic crust origin (e.g., MORB, ophiolite). According to the classification and regression tree analysis proposed by Belousova et al. (2002), the rock types from which the detrital zircon crystallized are dominated by granitoid, dolerite, basalt, and carbonatite (Fig. 9d).

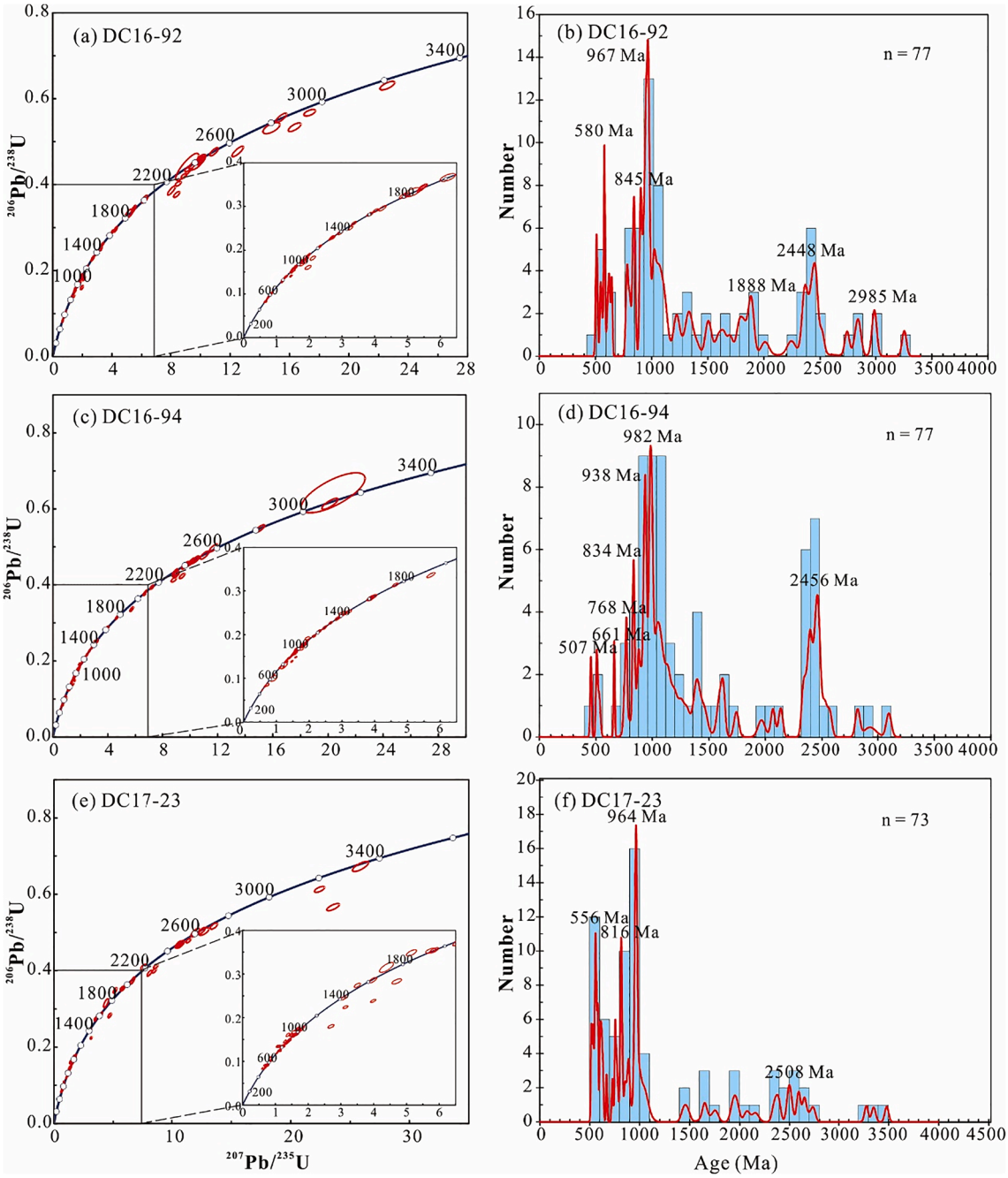

Fig. 6. Concordia plots (left column) and relative probability plots (right column) for detrital zircon U-Pb ages in our samples.

5. Discussion

5.1. Constraints on depositional age of the sedimentary successions

5.1.1. Age reassignment for the Qiasi Group

Depositional age of the Qiasi Group has long been controversial. It is traditionally considered to be Paleoproterozoic based on whole-rock Rb-Sr isochron age (1972 ± 289 Ma; n = 3) and regional stratigraphic correlation (Du, 1986; BGMRSP, 1991; Li et al., 1991). However, a recent study shows that the *meta*-volcanic/sedimentary rocks from the 2nd and 3rd members of Qiasi Group were formed at Neoproterozoic (Tian, 2020). The 4th member of Qiasi Group has the largest exposure area among the four members (Fig. 2a), but its depositional age is still equivocal.

In this study, zircons of three sandstone samples from the 4th member of Qiasi Group have the youngest $^{206}Pb/^{238}U$ ages of 510 ± 8.6 Ma (DC16-92), 456 ± 6.6 Ma (DC16-94), and 515 ± 4.8 Ma (DC17-23), respectively (Table 1). Although the youngest zircon from sample DC16-94 is considerably younger than that from the other two samples, the sampling sites are close to each other, and thus the three samples should have received similar detritus and deposited after 456 Ma. However, the minimum depositional age is difficult to constrain due to the paucity of volcanic rock interlayer and intruding pluton. Although some zircon grains develop metamorphic rims with strong CL reflectance, these rims are too narrow to be LA-ICP-MS U-Pb dated (Fig. 4). Previous studies found that the Qiasi Group (4th member) contains macroalgal fossils *Trachysphaereridium* sp. (Du, 1986; BGMRSP, 1991) that lived from the Mesoproterozoic to early Devonian (Zhu et al., 1984; Gong et al., 2009),

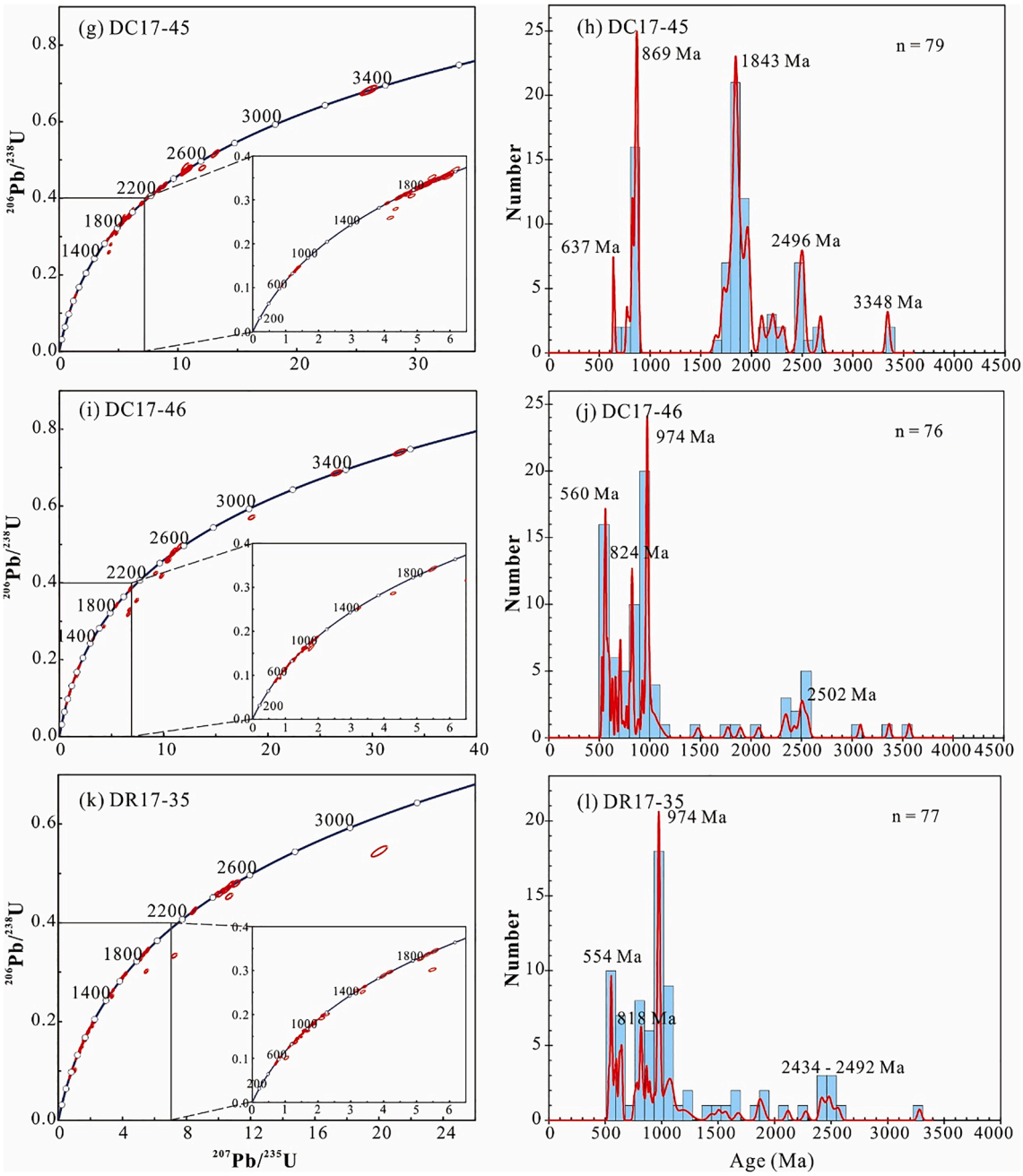

Fig. 6. (*continued*).

indicating that the deposition should not have continued after the early Devonian. Moreover, the lower Devonian strata locally overlie the Qiasi Group (4th member) along an angular unconformity in our study area. The youngest detrital zircons (515 – 456 Ma), combined with paleontological and geological evidence, indicate that the Qiasi Group (4th member) was probably deposited in the late Ordovician to Silurian (ca. 456 – 419 Ma). In summary, we suggest that the 2nd and 3rd members of the Qiasi Group were deposited in middle Neoproterozoic, and the 4th member was deposited in late Ordovician to Silurian.

5.1.2. Cambrian strata

Sample DR17-35 was collected from the well-defined lower Cambrian strata (Zhongza Town, western Yidun Terrane), with its youngest detrital zircon (532 ± 7.9 Ma) defining the maximum depositional age. Given that the strata are overlain by the lower Ordovician strata, it should be deposited at ca. 532 – 485 Ma, which agrees with the previously-assigned Cambrian age based on fossils and stratigraphic correlation (Zheng et al., 1984).

Sample DC17-45 was taken from the previously-defined (based on stratigraphic correlation) Cambrian strata in the eastern Yidun Terrane. Our LA-ICP-MS U-Pb dating yielded the youngest zircon age of 637 ± 5 Ma, which represents the maximum depositional age of the sample. The sample contains two major detrital zircon age populations of 821 – 890 Ma (peak ~ 869 Ma) and 1714 – 1977 Ma (peak ~ 1843 Ma), which is distinct from the Cambrian sample DR17-35 in the western Yidun Terrane (Fig. 6h and l). In contrast, except for the proportion of specific age population, the detrital zircon age populations of sample DC17-45 are comparable to those of the upper Neoproterozoic sedimentary sequence (e.g., Shigu Group) in the Yidun Terrane (Su et al., 2019) and the nearby Yangtze Block (e.g., Doushantuo and Chengjiang formations, Mengdong Group) (Fig. 10a and b). In this case, one possibility is that the previously-defined Cambrian strata in the eastern Yidun Terrane

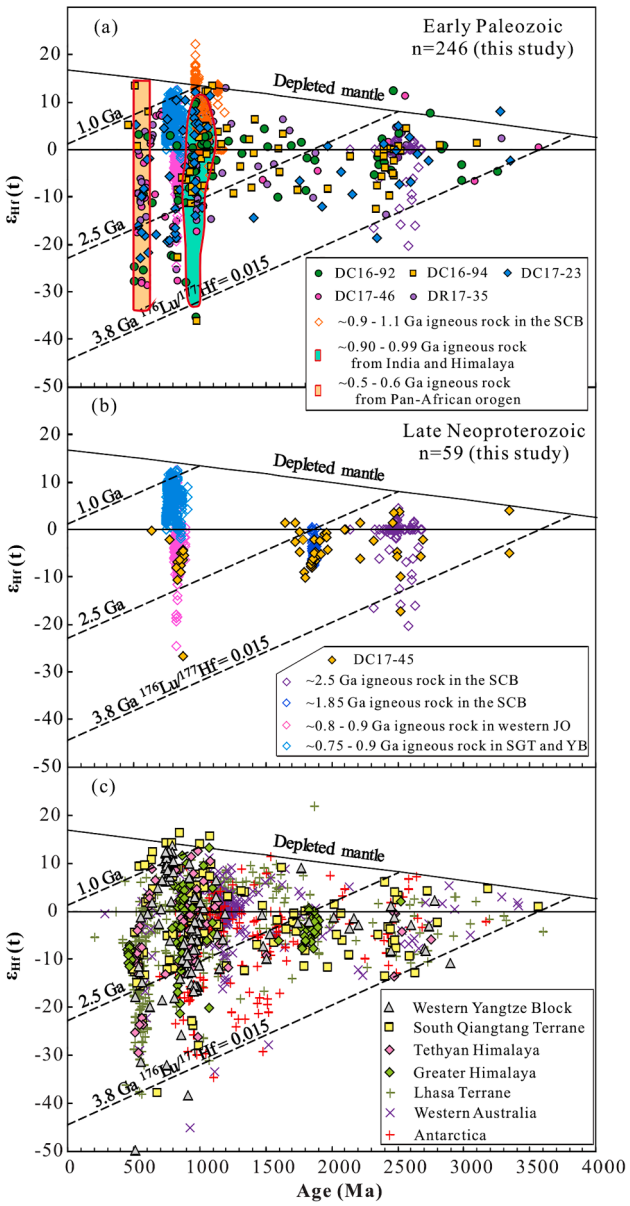

Fig. 7. Plots of εHf(t) versus U-Pb ages of detrital zircons from the (a) lower Paleozoic, and (b) upper Neoproterozoic sedimentary rocks in the Yidun Terrane. Detrital zircon data from the western Yangtze Block (Duan et al., 2011; Chen et al., 2016), South Qiangtang Terrane (Dong et al., 2011; Zhu et al., 2011a), Tethyan Himalaya (Zhu et al., 2011a), Greater Himalaya (Spencer et al., 2012), Lhasa Terrane (Zhang et al., 2008; Zhu et al., 2011a), western Australia (Veevers et al., 2005), and Antarctica (Grew et al., 2012; Halpin et al., 2013) are shown for comparison. Other data source for the South China Block (SCB): ~2.5 Ga igneous rocks (Zheng et al., 2006; Hu et al., 2013), ~1.85 Ga igneous rocks (Peng et al., 2009, 2012; Yu et al., 2009), ~0.9 – 1.1 Ga igneous rocks (Zhang et al., 2012a; Li et al., 2013a, 2018; Wang et al., 2013b, 2014b; Chen et al., 2014b, 2018b, 2021a; Zhu et al., 2016); western Jiangnan Orogen (JO): ~0.8 – 0.9 Ga igneous rocks (Wang et al., 2006, 2011b; Zheng et al., 2007; Zhao et al., 2013a; Yao et al., 2014a; Lv et al., 2021); Songpan-Ganze Terrane (SGT) and western Yangtze Block (YB): ~0.75 – 0.9 Ga igneous rocks (Zheng et al., 2007; Huang et al., 2008, 2009; Zhao et al., 2008a, 2008b, 2010a; Chen et al., 2015; Meng et al., 2015; Luo et al., 2018; Zhu et al., 2019a, 2019b). The fields of 0.9 – 0.99 Ga igneous rocks from India-Himalaya and 0.5 – 0.6 Ga igneous rocks from the Pan-African Orogen are modified after Liu et al. (2020).

were deposited in the late Neoproterozoic. Another possibility is that the strata were deposited in the Cambrian but shared similar detrital provenance to those of the upper Neoproterozoic sequences. Given that sample DR17-35 was collected from the well-defined Cambrian strata, which has markedly different detrital zircon age patterns from sample DC17-45, and that the previously-assigned Cambrian strata are distributed around the Sinian strata in the region (Fig. 2a), it is most likely that these previously-assigned Cambrian sedimentary rocks in the eastern Yidun Terrane were actually deposited in the late Neoproterozoic.

5.2. Detrital zircon provenance

5.2.1. The upper Neoproterozoic strata

Zircon grains from the upper Neoproterozoic sedimentary rocks in the Yidun Terrane contain a high proportion of late Paleoproterozoic (1714 – 1977 Ma; peak ~ 1843 Ma) and middle Neoproterozoic (821 – 890 Ma; peak ~ 869 Ma) zircons, and fewer late Archean to early Paleoproterozoic (2317 – 2520 Ma; peak ~ 2496 Ma) ones (Fig. 10a). These three age ranges match well with the multiphase magmatic events in the neighboring South China Block. This implies that the South China Block was probably the main detrital source for the upper Neoproterozoic sedimentary rocks in the Yidun Terrane. The minor population of 2317 – 2520 Ma detrital zircons were likely sourced from the late Archean-early Paleoproterozoic magmatic rocks (e.g., ~2500 Ma Douling Complex; Hu et al., 2013) in the northern margin of Yangtze Block. Such inference is supported by their overlapping $\varepsilon_{Hf(t)}$ values and crustal model ages (Fig. 7b). The 1714 – 1977 Ma zircons are broadly consistent with the ~ 1850 Ma Quanqitang granitic pluton and mafic dykes in the northern Yangtze Block (Peng et al., 2009, 2012), and with the 1860 – 1890 Ma granitoids in the northeastern Cathaysia Block (Yu et al., 2009). Similar zircon Hf isotope compositions and crustal model ages further support such interpretation (Fig. 7b). Alternatively, the 1714 – 1977 Ma and 2317 – 2520 Ma zircons could also be sourced from the recycling of Paleoproterozoic-Mesoproterozoic strata (e.g., Dahongshan, Dongchuan, and Hekou groups) in the western Yangtze Block, which contain a high population of ~ 1700 – 1900 Ma and ~ 2300 – 2400 Ma detrital zircons (Fig. 11c). The nearby Songpan-Ganze Terrane, Yangtze Block, and Jiangnan Orogen all contain voluminous 870 – 730 Ma igneous rocks, and may represent the possible source for the 821 – 890 Ma detrital zircons. Nonetheless, Neoproterozoic igneous rocks in this age range from the Songpan-Ganze Terrane and western/northern margin of the Yangtze Block have mostly positive zircon $\varepsilon_{Hf(t)}$ values (Fig. 7b), different from the 821 – 890 Ma detrital zircons in upper Neoproterozoic strata in the Yidun Terrane that has exclusively negative $\varepsilon_{Hf(t)}$ values (Fig. 7b). The scarcity of Neoproterozoic detritus from the Songpan-Ganze Terrane and western/northern margin of the Yangtze Block may suggest that the Neoproterozoic magmatic rocks were not exposed (and eroded) at that time. This agrees with the widely-accepted interpretation that most domains of the Yangtze Block were submerged during much of the Ediacaran (Yao et al., 2014. and references therein). Alternatively, the western Jiangnan Orogen, which contains voluminous Neoproterozoic plutons with negative $\varepsilon_{Hf(t)}$ values (Fig. 7b), may represent possible provenance for the 821 – 890 Ma detrital zircons.

5.2.2. The lower Paleozoic strata

As above mentioned, five early Paleozoic samples have similar detrital zircon age ranges and populations at 2600 – 2300 Ma, 1100 – 900 Ma, 900 – 740 Ma, and 690 – 480 Ma, with peaks at ~ 2480 Ma, 974 Ma, ~822 Ma, and ~ 554 Ma (Fig. 10d). In the Yidun Terrane, apart from the ~ 822 Ma *meta*-rhyolite and minor 991 – 775 Ma detrital zircon reported from the Qiasi Group (2nd and 3rd members) (Tian, 2020), no other coeval igneous rocks or detrital zircons in sedimentary rocks were reported. Moreover, most detrital zircons in the lower Paleozoic sedimentary rocks are rounded to subrounded (Fig. 4), suggesting long-distance transport before their deposition (Chen et al., 2018a). Hence,

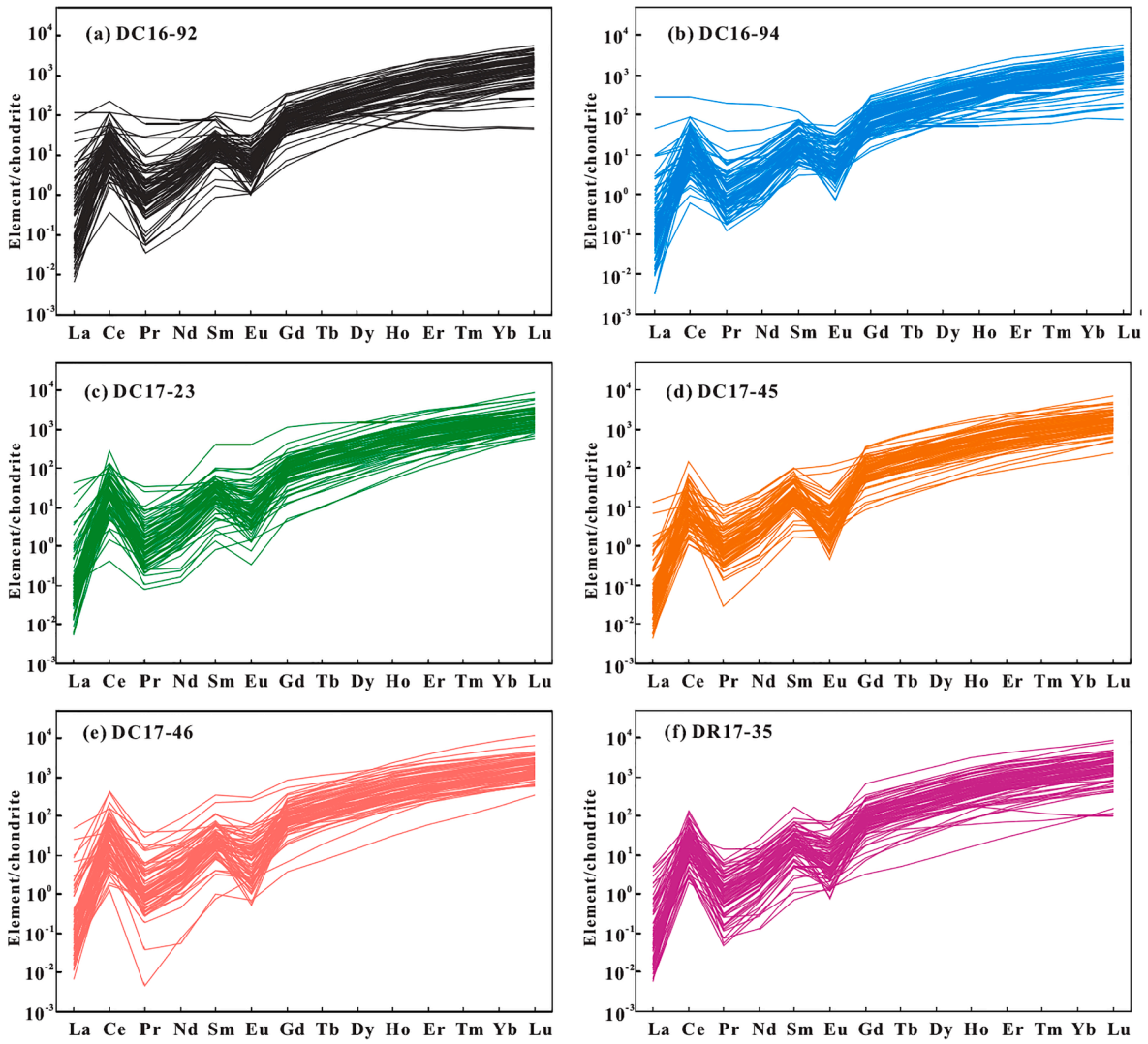

Fig. 8. Chondrite-normalized rare earth element (REE) patterns for the analyzed detrital zircons. Chondrite-normalizing values are from Sun and McDonough (1989).

most detritus in the lower Paleozoic sedimentary rocks in the Yidun Terrane may have sourced from exotic terranes.

As previously mentioned, the neighboring Yangtze Block contains late Archean to early Paleoproterozoic magmatic rocks, such as ~ 2500 Ma Douling Complex (Hu et al., 2013), and ~ 2700 – 2500 Ma Yudongzi Complex (Chen et al., 2019, and references therein), and ~ 2360 – 2220 Ma Cuoke Complex (Cui et al., 2020; Lu et al., 2021). These Neoarchean-early Paleoproterozoic magmatic rocks could be the detrital source of 2600 – 2300 Ma zircons. This inference is supported by the similar zircon $\varepsilon_{Hf(t)}$ values and crustal model ages between them (Fig. 7a).

The late Mesoproterozoic-early Neoproterozoic (1100 – 900 Ma) detrital zircons constitute the most abundant age population in our lower Paleozoic samples, which corresponds temporally to the global Grenville orogeny associated with the final Rodinia supercontinent assembly (Hoffman, 1991). The adjacent South China Block contains local outcrops of 1100 – 900 Ma igneous rocks (Zhang et al., 2012a; Li et al., 2013a, 2018; Wang et al., 2013b, 2014b; Chen et al., 2021a), which may supply some detritus for the lower Paleozoic sedimentary rocks in the Yidun Terrane. However, Grenville-age magmatic rocks in South China Block are volumetrically minor and mainly mafic, and thus may not be able to supply such enough detrital zircons of this age range. Furthermore, detrital zircon trace element compositions reveal that, in addition to basic rocks, the detrital sources also contain abundant granitoids and carbonatites (Fig. 9d). Most importantly, the 1100 – 900 Ma detrital zircons from the Yidun Terrane have both negative and positive $\varepsilon_{Hf}(t)$ values (Fig. 7a), distinct from magmatic zircons from similar-age igneous rocks in South China Block, which have dominantly positive $\varepsilon_{Hf(t)}$ values (Fig. 7a). Most 1100 – 900 Ma detrital zircons are moderately- to highly-rounded, indicating that they have experienced recycling or long-distance transport before deposition. However, a recycling origin can easily be ruled out, as the middle and upper Neoproterozoic strata in both the Yidun Terrane, and nearby Songpan-Ganze Terrane and Yangtze Block do not develop 1100 – 900 Ma detrital zircons (Figs. 10 and 11). The lower Neoproterozoic strata (e.g., Kunyang and Huili groups) in the Yangtze Block have a small amount of ~ 990 Ma detrital zircons, but a large amount of ~ 1850 Ma ones (the latter being uncommon in our lower Paleozoic sedimentary rocks) (Fig. 11b). Therefore, we suggest that South China Block is not the main detrital source of the 1100 – 900 Ma zircons. In other words, other exotic terranes may have been connected to the Yidun Terrane in the early Paleozoic and supplied the 1100 – 900 Ma zircons.

For the 900 – 740 Ma detrital zircons, some of them have euhedral to subhedral profiles, which indicates little transport before deposition, e.g., from the nearby Songpan-Ganze Terrane and South China Block. Unlike the upper Neoproterozoic strata in the Yidun Terrane, which are dominated by sedimentary input from Neoproterozoic magmatic rocks

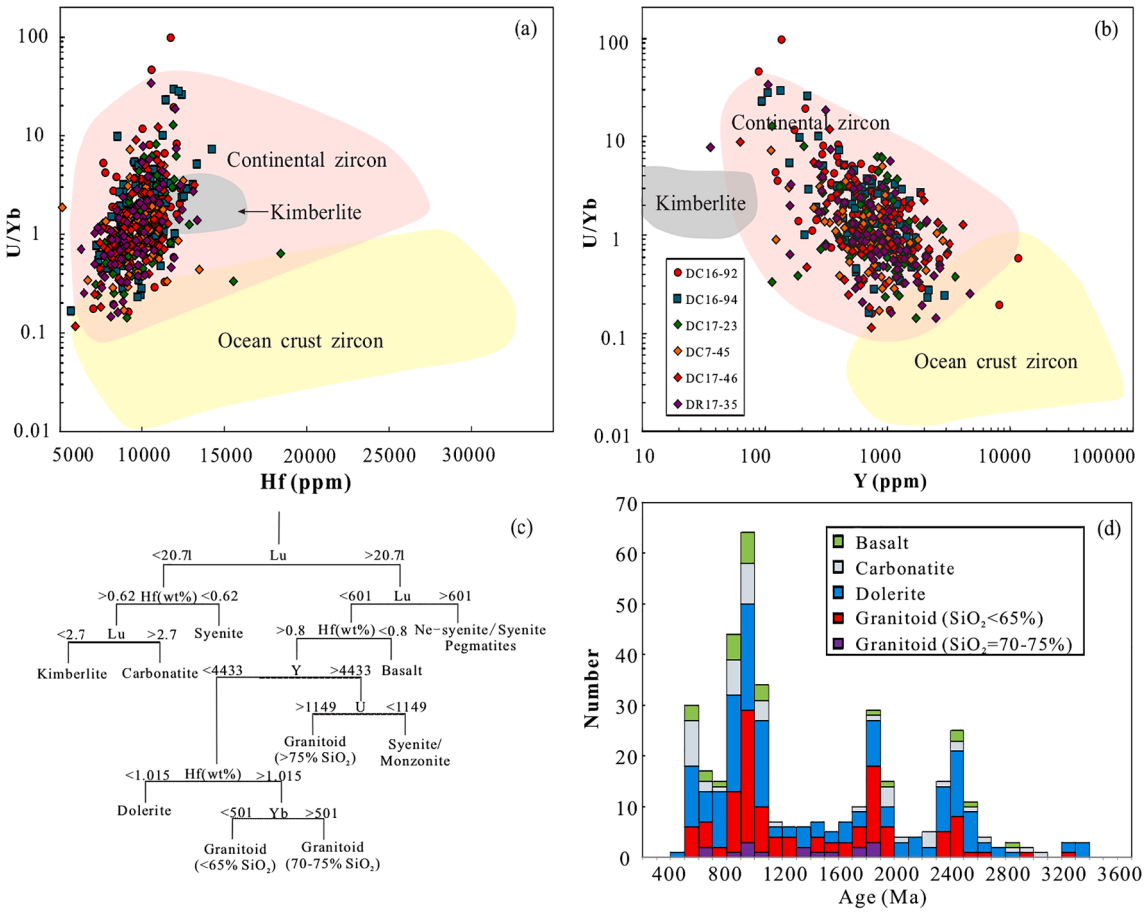

Fig. 9. Geochemical discriminant diagrams for detrital zircons in our samples. (a) Hf vs. U/Yb diagram (after Grimes et al., 2007); (b) Y vs. U/Yb diagram (after Grimes et al., 2007); (c) Classification and regression trees for the recognition of zircon from different source rock types (Belousova et al., 2002); (d) Inferred parent rock types of detrital zircon are based on their trace element compositions.

in the western Jiangnan Orogen. The 900 – 740 Ma zircons from the lower Paleozoic strata exhibit both negative and positive $\varepsilon_{Hf(t)}$ values (Fig. 7a), suggesting an additional detrital input from the Yangtze Block. Moreover, the source-proximal middle Neoproterozoic siliciclastic rocks in the Yidun Terrane, Songpan-Ganze Terrane, and Yangtze Block also contain a large proportion of middle Neoproterozoic zircons (Fig. 11a), which may also have contributed to the 900 – 740 Ma detritus.

The late Neoproterozoic-Cambrian (690 – 480 Ma) detrital zircons are the second-most abundant age population in our early Paleozoic samples. Apart from a few late Neoproterozoic volcanic intercalations, coeval magmatic rocks are rare in the Yidun Terrane and the neighboring Yangtze Block and Songpan-Ganze Terrane. Although the Cathaysia Block develops early Paleozoic granites (460 – 400 Ma) that were formed under an intracratonic orogeny setting (e.g., Zhang et al., 2012b; Zhao et al., 2013b; Huang and Wang, 2019), these rocks have much younger emplacement ages than the zircon grains under discussion, precluding the Cathaysia Block as a possible contributor. Here, we interpret that these late Neoproterozoic-early Paleozoic detrital zircons were also sourced from an exotic terrane that was once connected to the Yidun Terrane during the early Paleozoic.

Numerous studies reveal that prominent end-Mesoproterozoic to earliest Neoproterozoic and late Neoproterozoic-early Paleozoic detrital zircon populations are common in many siliciclastic suites in East Gondwana (Myrow et al., 2010; Duan et al., 2011; Cawood et al., 2013; Xu et al., 2013; Xue et al., 2021). In the Gondwana, there are abundant end-Mesoproterozoic to earliest Neoproterozoic igneous rocks along the Rayner-Eastern Ghats (990 – 900 Ma) belt in India and Antarctica, and along the Maud-Namaqua-Natal (1090 – 1030 Ma) belt in Antarctica and Africa (e.g., Fitzsimons, 2000). Similarly, late Neoproterozoic to early Paleozoic igneous rocks related to the final Gondwana assembly and related orogeny are extensively documented in the East Gondwana (e.g., Meert, 2003), e.g., 600 – 500 Ma and 560 – 530 Ma igneous rocks along the Prydz-Darling and Kuunga orogen, respectively. The distinct 974 Ma and 554 Ma detrital zircon age peaks from the lower Paleozoic sedimentary rocks in the Yidun Terrane correlate well with many Grenvillian and Pan-African magmatic rock suites in the East Gondwana. Therefore, we consider that the East Gondwana is the most likely source of the Grenvillian and Pan-African zircon populations. This inference is further supported by their similar $\varepsilon_{Hf(t)}$ values (Fig. 7a).

In summary, the 2600 – 2300 Ma and 900 – 740 Ma detrital zircons could be supplied by coeval igneous rocks in the neighboring Songpan-Ganze Terrane and South China Block, while the 1000 – 900 Ma and 690 – 480 Ma zircons are likely derived from the East Gondwana (e.g., Rayner-Eastern Ghats, Prydz-Darling, and Kuunga orogens).

5.3. *Tectonic affinity of the late Neoproterozoic-early Paleozoic Yidun Terrane*

The Yidun Terrane was long considered to be the western extension of the Yangtze Block, in view of their similar Neoproterozoic-Paleozoic lithological assemblages and fossils (BGMRSP, 1991). The Yidun Terrane may have rifted from the Yangtze Block due to the late Permian Emeishan mantle plume activity (Chang, 2000; Song et al., 2004; Xiao et al., 2004). However, some authors argued that the Yidun Terrane was rifted from the eastern Kunlun Terrane in the early Triassic, due to back-arc extension of the north-dipping Paleo-Tethyan subduction (Pullen

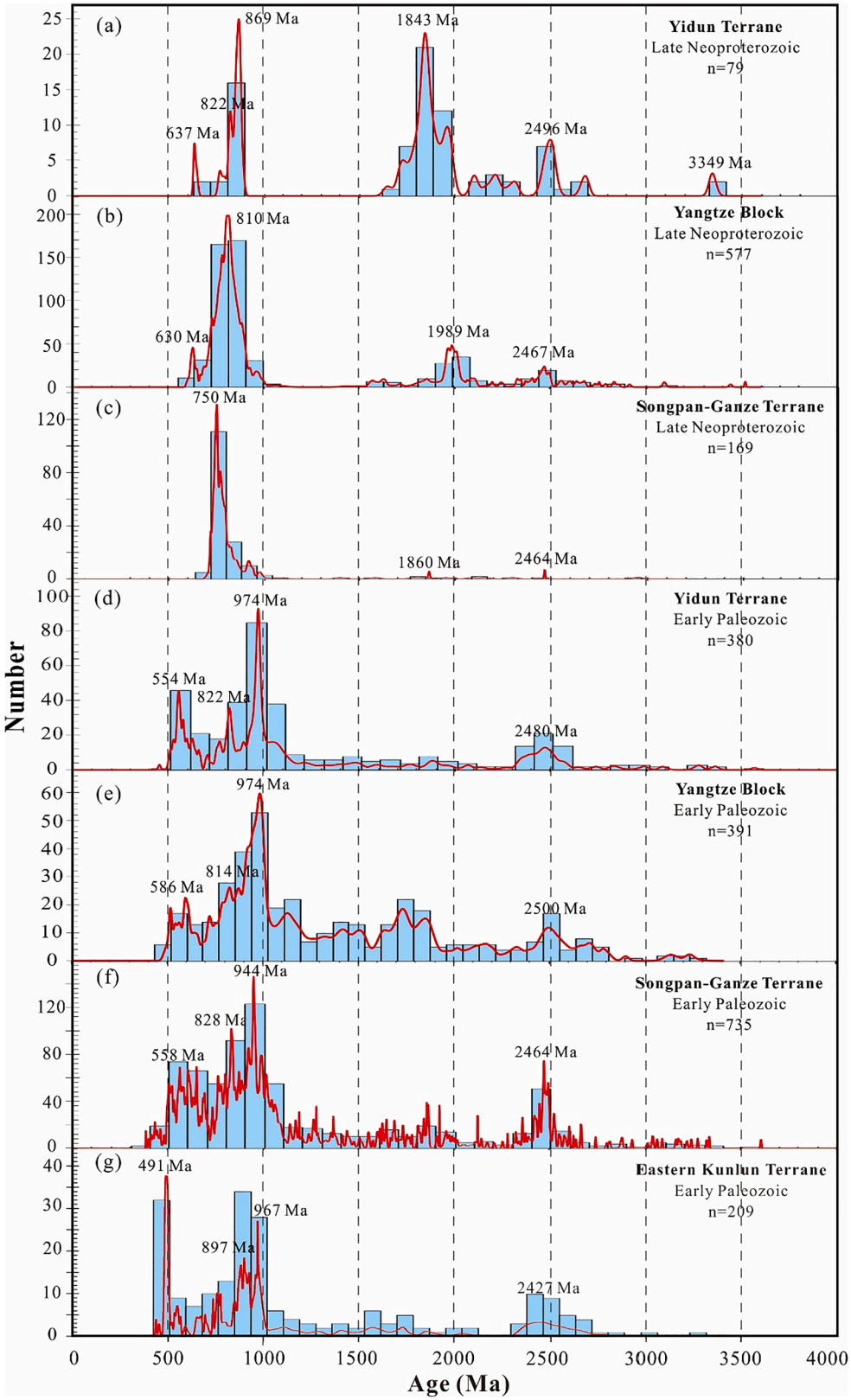

Fig. 10. Detrital zircon age distribution spectra for the upper Neoproterozoic and lower Paleozoic sedimentary rocks in the Yidun Terrane, Yangtze Block, Songpan-Ganze Terrane, and eastern Kunlun Terrane. All detrital zircon U-Pb ages are within 90% concordance. Data sources: (a) Upper Neoproterozoic clastic rocks in the Yidun Terrane (this study); (b) Upper Neoproterozoic clastic rocks in the Yangtze Block (Liu et al., 2008a; Sun et al., 2009; Zhou et al., 2018); (c) Upper Neoproterozoic clastic rocks in the Songpan-Ganze Terrane (Chen et al., 2016, 2018a); (d) Lower Paleozoic clastic rocks in the Yidun Terrane (this study); (e) Lower Paleozoic clastic rocks in the Yangtze Block (Wang et al., 2010; Duan et al., 2011; Zhou et al., 2018); (f) Lower Paleozoic clastic rocks in the Songpan-Ganze Terrane (Chen et al., 2016, 2018a); (g) Lower Paleozoic clastic rocks in the eastern Kunlun Terrane (Jin et al., 2015; Peng et al., 2017; Yan et al., 2017).

et al., 2008; Ding et al., 2013; Zhang et al., 2014b). Recently, Tian (2020) suggested that the middle Neoproterozoic *meta*-sedimentary rocks (collected from the 3rd member of the Qiasi Group) in Yidun Terrane have similar detrital zircon age population to those of the Neoproterozoic strata in the Yangtze Block, but are distinct from coeval strata in the eastern Kunlun Terrane. This demonstrates a close tectonic link between the Yidun Terrane and Yangtze Block in the middle Neoproterozoic. Our late Neoproterozoic sample is characterized by the presence of obvious age peaks at ~ 637 Ma, ~822 Ma, ~869 Ma, ~1843 Ma, and ~ 2496 Ma, similar to those of upper Neoproterozoic strata in

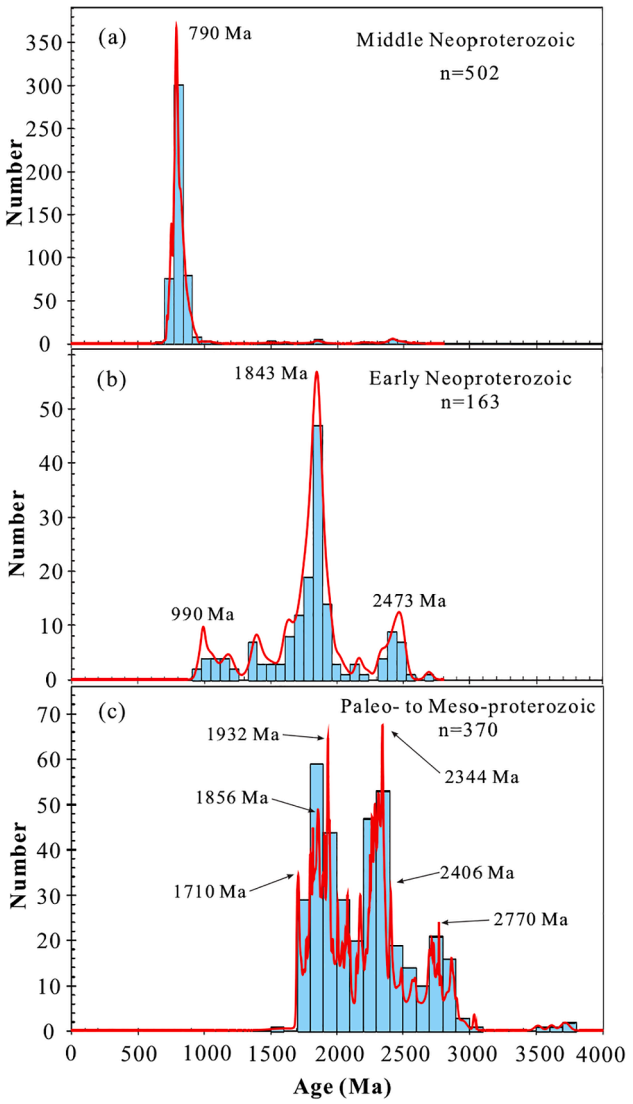

Fig. 11. Detrital zircon U-Pb age probability plots for the Paleo-/Meso-proterozoic, and lower/middle Neoproterozoic siliciclastic rocks in the Yidun and Songpan-Ganze terranes, and Yangtze Block. All detrital zircon U-Pb ages are within 90% concordance. Data source: Paleo-/Meso-Proterozoic rocks are from Greentree and Li. (2008), Zhao et al. (2010b), Chen et al. (2013), and Wang and Zhou. (2014), lower Neoproterozoic rocks are from Sun et al. (2009), middle Neoproterozoic rocks are from Sun et al. (2009), Chen et al. (2016), Zhu et al. (2018), and Tian. (2020).

the western Yangtze Block (Fig. 10b). Moreover, the sedimentary rock types (e.g., algae dolomite) and fossils (e.g., *Balios pinguensis*, *Paleomicrocystis*, *Tortifimbria*) of the upper Neoproterozoic Yidun Terrane and Yangtze Block are comparable (Du, 1986), suggesting a close linkage between these two terranes until then. Besides, provenance analysis shows that detritus of the upper Neoproterozoic sandstone in the Yidun Terrane were mainly sourced from the nearby South China Block, further supporting that the Yidun Terrane was part of the Yangtze Block in the late Neoproterozoic.

Detrital zircons from lower Paleozoic sedimentary rock in the Yidun and eastern Kunlun terranes show overall comparable age distributions, but there are still noticeable differences. For instance, the Yidun Terrane has a major age peak at ~ 974 Ma and two subordinate peaks at ~ 554 Ma and ~ 822 Ma (Fig. 10d), whereas the eastern Kunlun Terrane contains the main age peak at ~ 491 Ma and subordinate peaks at ~ 967 Ma and ~ 897 Ma (Fig. 10g). By contrast, the Yidun Terrane has more similar detrital zircon age spectra to coeval rocks in the Yangtze Block (Fig. 10e), suggesting a potential tectonic affinity between them. Such an inference is further supported by the following observations. (1) In the early Paleozoic, the eastern Kunlun Terrane have experienced extensive subduction- accretionary orogeny and formed plenty of subduction-related igneous rocks, such as diorite (408 – 447 Ma), granodiorite (439 – 441 Ma), and adakitic intrusions (454 – 402 Ma) (Song et al., 2013; Zhang et al., 2014a; Dong et al., 2018. and references therein). This is in good agreement with the presence of abundant early Paleozoic detrital zircons in eastern Kunlun Terrane lower Paleozoic sediments. However, early Paleozoic magmatism is absent within the Yidun Terrane, as well as in the neighboring Songpan-Ganze Terrane and Yangtze Block. (2) The eastern Kunlun Terrane had undergone amphibolite-to granulite- (locally eclogite-) facies metamorphism in the early Paleozoic, due to the deep-subduction of the Kunlun Ocean (Liu et al., 2005; Meng et al., 2013; Dong et al., 2018). In contrast, the lower Paleozoic strata in the Yidun Terrane only experienced greenschist-facies metamorphism (Tian et al., 2018a, 2018b), similar to coeval strata in the western Yangtze Block (BGMRSP, 1991; Yan et al., 2008). (3) Lower Paleozoic sedimentary rocks in the eastern Kunlun Terrane were formed in an active continental margin setting (Chen et al., 2014c; Dong et al., 2018), whereas in the Yidun Terrane and western Yangtze Block were deposited in a passive continent margin setting (BGMRSP, 1991; Tian, 2020). (4) Detrital zircons from lower Paleozoic sedimentary rocks in both the Yidun Terrane and Yangtze Block have similar $\varepsilon_{Hf(t)}$ values (Fig. 7a and c), demonstrating that they shared a uniform detrital provenance. Based on the above considerations, we suggest that the Yidun Terrane still has a close tectonic affinity to the Yangtze Block in the early Paleozoic, rather than the eastern Kunlun Terrane.

5.4. *Paleogeographic position of the Yidun Terrane in East Gondwana*

As above mentioned, most terranes in the Tibetan Plateau were separated from the East Gondwana, yet any tectonic link between the Yidun Terrane and Gondwana remains enigmatic. In this study, our early Paleozoic samples have prominent end-Mesoproterozoic to earliest Neoproterozoic (ca. 1100 – 900 Ma) and late Neoproterozoic to Cambrian (ca. 690 – 480 Ma) detrital zircon age populations, indicating a spatial link between the Yidun Terrane and East Gondwana. To further constrain the paleogeographic position of Yidun Terrane in the East Gondwana, detrital zircons from age-equivalent sequences in South Qiangtang Terrane, northeastern India (including the Tethyan-, Greater-, and Lesser Himalaya), northwestern India, Lhasa Terrane, East Antarctica, and western/NE/SE Australia are compiled for comparison (Fig. 12). The results show that detrital zircons from East Antarctica, Australia, and Lhasa Terrane show prominent age peaks at ~ 1040 – 1170 Ma (Fig. 12h-k), which are absent in our lower Paleozoic sedimentary rocks. This difference suggests that the Yidun Terrane was not likely connected to Australia, East Antarctica, or Lhasa Terrane, where abundant late Mesoproterozoic magmatic rocks are emplaced along the Namaqyua-Natal Orogen (1090 – 1030 Ma) and the Wilkes-Albany-Fraser Orogen (1330 – 1130 Ma) (Fig. 13). If the Yidun Terrane was located next to Australia or Antarctica, distinct ~ 1040 – 1170 Ma age peaks would be present in the Yidun Terrane detrital zircon age spectra. The presence of pronounced 1700 – 1800 Ma detrital zircon age peaks in the lower Paleozoic strata in the Lesser Himalaya and northwestern India (but absent in the Yidun Terrane) (Fig. 12e and f) implies that the Yidun Terrane was not located next to these terranes either. In contrast, the distinctive 974 Ma detrital zircon age peak is found in both the Yidun Terrane and similar-aged siliciclastic rocks from the South Qiangtang, Tethyan Himalaya, and Greater Himalaya terranes (Fig. 12a–d). suggesting that they were proximal to each other and shared a common detrital provenance in the early Paleozoic. Accordingly, we consider that the Yidun Terrane was geographically close to the northeastern India (Tethyan- and Greater Himalaya) and the Qiangtang Terrane in the early Paleozoic. This interpretation is further supported by that the detrital zircons from both places have nearly identical $\varepsilon_{Hf(t)}$ values (Fig. 7c).

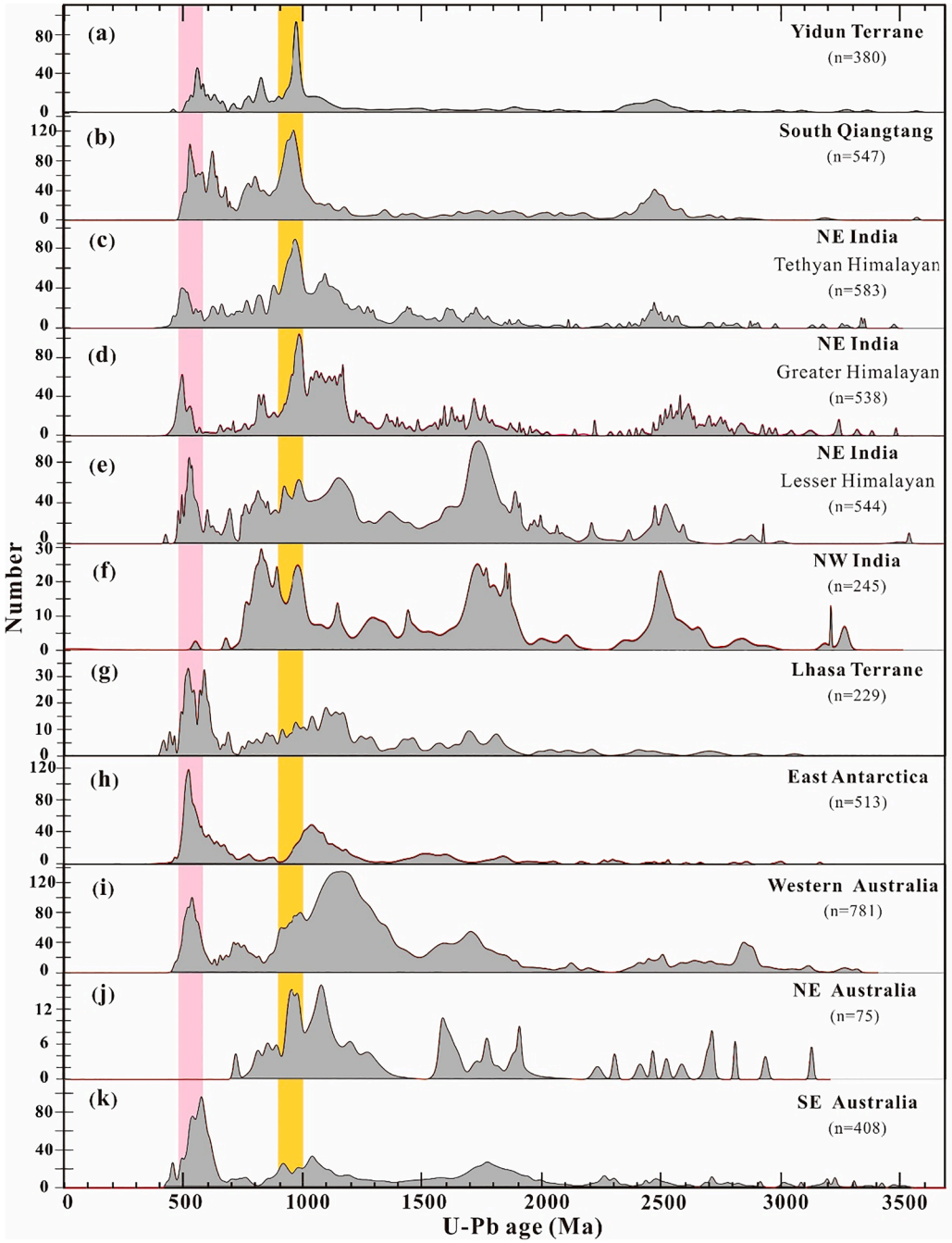

Fig. 12. Relative probability plots of detrital zircon U-Pb age from the lower Paleozoic sedimentary rocks in the (a) Yidun Terrane (this study), (b) South Qiangtang Terrane (Pullen et al., 2008; Dong et al., 2011; Zhu et al., 2011a), (c) Tethyan Himalaya (Myrow et al., 2009, 2010; Hughes et al., 2011; McQuarrie et al., 2013), (d) Greater Himalaya (Gehrels et al., 2006a, 2006b; McQuarrie et al., 2013), (e) Lesser Himalaya (McQuarrie et al., 2008, 2013; Myrow et al., 2010; Hofmann et al., 2011; Long et al., 2011), (f) northwestern India Craton (Turner et al., 2014; Wang et al., 2019), (g) Lhasa Terrane (Zhang et al., 2008; Dong et al., 2009, 2010), (h) East Antarctica (Goodge et al., 2002, 2004a, 2004b), (i) western Australia (Cawood and Nemchin, 2000; Markwitz et al., 2017), (j) northeastern Australia (Fergusson et al., 2001, 2007), and (k) southeastern Australia (Ireland et al., 1998; Berry et al., 2001).

Recently, lines of evidence (including geologic, paleomagnetic, and faunal data) support that the South China Block (including the Yangtze and Cathaysia blocks) was also located on the northern margin of East Gondwana in the early Paleozoic (Cawood et al., 2013; Xu et al., 2013; Chen et al., 2016, 2018a, 2021b; Wang et al., 2021). Such paleogeographic reconstruction is consistent with the provenance discrimination that both South China Block and East Gondwana supplied detritus to the Yidun Terrane during the deposition of lower Paleozoic sediments.

5.5. *Tectonic evolution for the late Neoproterozoic to late Paleozoic Yidun Terrane*

As shown in Fig. 10, the upper Neoproterozoic-lower Paleozoic sedimentary rocks in both the Yangtze Block and Yidun-Songpan-Ganze terranes have comparable detrital zircon age populations, indicating that they were connected to each other and experienced similar tectonic evolution during late Neoproterozoic to early Paleozoic periods. Provenance analysis further suggests that upper Neoproterozoic siliciclastic rocks in both the Yidun-Songpan-Ganze terranes, as well as Yangtze Block, were sourced from the interior of South China (Zhou et al., 2018; Su et al., 2019; Chen et al., 2021b; this study). Such a self-sufficient sedimentary operation is accordant with paleogeographic reconstruction that South China Block was isolated in the Proto-Tethys Ocean during late Cryogenian to early Ediacaran (~700 – 600 Ma) (Zhao et al., 2018). However, abundant Greenville and Pan-African detrital zircons from the East Gondwana were imported into the early Paleozoic sedimentary rocks in the Yidun-Songpan-Ganze terranes and Yangtze Block (Fig. 10). This shift of sediment provenance indicates significant tectonic and paleogeographic location change of the Yidun-Songpan-Ganze terranes and Yangtze Block, which could be best ascribed to the collision

Fig. 13. Schematic tectonic evolution model of Yidun Terrane during (a) late Cryogenian-early Ediacaran, (b) late Ediacaran-Silurian, and (c) early Devonian periods (modified after Fitzsimons, 2000; Boger et al., 2001; Xu et al., 2013; Wang et al., 2021). Locations of South Qiangtang and Lhasa terranes are from Zhu et al. (2011) and Zhao et al. (2017), respectively. The inferred pathway of sediments is from Myrow et al. (2010) and Chen et al. (2018). CB: Cathaysia Block; GH: Greater Himalaya; LH: Lesser Himalaya; SQT: South Qiangtang Terrane; TH: Tethyan Himalaya; YB: Yangtze Block; YT: Yidun Terrane. Terrane outlines are not to scale.

between Yidun-Songpan-Ganze terranes, Yangtze Block, and East Gondwana in the late Neoproterozoic-early Cambrian (ca. 570 – 520 Ma). A possible collision between Yidun and Songpan-Ganze terranes, Yangtze Block, and East Gondwana is supported by the following evidence: (1) the Yidun Terrane experienced regional metamorphism during ca. 570 – 520 Ma (Su et al., 2019. and references therein), and coeval metamorphism was also recorded in the Tethyan Himalaya (monazite $^{208}Pb/^{232}Th$ ages: 588 – 423 Ma) (Webb et al., 2011); These metamorphic events are consistent with the estimated collision timing (ca. 580 – 540 Ma) between South China Block and the East Gondwana (Yao et al., 2014b; Yang et al., 2020). (2) the western Yangtze Block develops Cambrian molasse-like sediments, and its detrital provenance was mainly derived from the ~ 580 – 500 Ma Cadomian arc along the northern margin of East Gondwana (Chen et al., 2021b). (3) voluminous 870 – 730 Ma igneous rocks in the western and northern margin of the Yangtze Block were submerged or buried at depth in the late Neoproterozoic, but then exhumed and eroded to provide detritus materials for the lower Paleozoic siliciclastic rocks (Yang et al., 2020; this study). This indicates that the margin of Yangtze Block experienced extensive tectonic uplift during the late Neoproterozoic to early Paleozoic transition period, possibly related to the collision of Yidun-Songpan-Ganze terranes and Yangtze Block with East Gondwana.

Integrating published data with our discussion above, we proposed the following model for the tectonic evolution of the late Neoproterozoic-early Paleozoic Yidun Terrane:

(1) After the Rodinia supercontinent breakup at ~ 720 Ma (Li et al., 2013c), the rifted Yidun-Songpan-Ganze terranes and Yangtze Block may be isolated in the Proto-Tethys Ocean, which blocked the detrital input from other cratons (e.g., India), and consequently received detritus only from their uplifted denudation zone (Fig. 13a). Meantime, the three terranes/block drifted from medium-high to low latitude (Li et al., 2013c; Zhou et al., 2018; Su et al., 2019; Tian, 2020), gradually approaching the northern margin of East Gondwana (Fig. 13a).

(2) At ~ 570 – 520 Ma, the Yidun-Songpan-Ganze terranes and Yangtze Block started to collide with the northern margin of Gondwana and receive abundant detritus from the E Ghats-Rayner, Kuunga, and Prydz-Darling orogens in the East Gondwana (Fig. 13b). Given that the Cambrian (ca. 532 – 485 Ma) and Ordovician-Silurian (ca. 456 – 419 Ma) sedimentary rocks have nearly identical detrital zircon age spectra, we suggest that these lower Paleozoic strata in the Yidun Terrane have largely the same provenance during their deposition. It is likely that the Yidun Terrane was not separated from the East Gondwana before the late Silurian. The Yidun Terrane and South China Block may have then rotated clockwise relative to the East Gondwana, leading to the final

Proto-Tethys closure (in a scissor-like pattern) and the formation of North India Orogen (ca. 530 – 470 Ma) along the northern margin of India Craton (Fig. 13b) (Cawood et al., 2007).

(3) Due to the late Silurian to early Devonian opening of the Paleo-Tethyan Jinshajiang-Ailaoshan oceans, the Yidun-Songpan-Ganze terranes and Yangtze Block were rifted away from the East Gondwana, and then drifted northward toward the southern Eurasian margin (Metcalfe, 2013, 2021; Lai et al., 2014a; Xia et al., 2016; Liu et al., 2018) (Fig. 13c). This is supported by the presence of late Early Devonian to middle Devonian deep-water radiolarian-bearing rocks in the Yidun Terrane (Zhang et al., 2000; Yang et al., 2010), and by the 383 – 362 Ma and 344 – 340 Ma ophiolites within the Jinshajiang and Ailaoshan ophiolitic mélanges, respectively (Wang et al., 2000; Jian et al., 2009). Tillites and glaciomarine faunas are developed in the upper Paleozoic strata of the Lhasa and Qiangtang terranes, and East Gondwana, but absent in the Yidun Terrane, Songpan-Ganze Terrane, and Yangtze Block. This also demonstrates that the Yidun-Songpan-Ganze terranes-Yangtze Block had separated from the East Gondwana at that time.

6. Conclusions

Based on detrital zircon U-Pb age and Hf isotopic data, we draw the following conclusions:

(1) The Qiasi Group (4th member) was deposited in the late Ordovician-Silurian (ca. 456 – 419 Ma), rather than the previously-believed age of Paleoproterozoic. The previously-assigned Cambrian strata in the eastern Yidun Terrane may have deposited in the late Neoproterozoic (after 637 Ma).
(2) Detritus for the upper Neoproterozoic clastic rocks were dominantly sourced from the nearby South China Block, whereas those for the lower Paleozoic clastic rocks were likely derived from Pan-African and Grenville-age provinces (e.g., Kuunga, Prydz-Darling, and E Ghats-Rayner orogens) in the East Gondwana, in addition to the Songpan-Ganze Terrane and South China Block.
(3) The Yidun Terrane has close tectonic affinity with the Yangtze Block during the late Neoproterozoic to early Paleozoic. In the early Paleozoic, the Yidun Terrane and Yangtze Block were located on the northern margin of East Gondwana, close to the Qiangtang, Tethyan Himalaya, and Greater Himalaya terranes.

CRediT authorship contribution statement

Zhen-Dong Tian: Writing – original draft, Investigation, Funding acquisition. **Cheng-Biao Leng:** Writing – review & editing, Funding acquisition, Project administration, Supervision. **Xing-Chun Zhang:** Writing – review & editing, Funding acquisition. **Feng Tian:** Formal analysis, Investigation. **Chun-Kit Lai:** Writing – review & editing.

Declaration of Competing Interest

The authors declare that they have no known competing financial interests or personal relationships that could have appeared to influence the work reported in this paper.

Acknowledgments

This study was financially supported by the Second Tibetan Plateau Scientific Expedition and Research (2021QZKK0301), National Natural Science Foundation of China (NSFC) grants (42102277, 42022021), and China Postdoctoral Science Foundation (2021 M703188). We thank Yanwen Tang for assisting with the LA-ICP-MS zircon U-Pb dating and trace element analyses, Hongfang Chen and Wei Gao for helping with the Hf isotope analyses, and Runsheng Yin for polishing the language of the paper. The authors thank Editor-in-Chief Wilson Teixeira and two anonymous reviewers for their very valuable and insightful comments, which greatly improved the quality of this paper.

Appendix A. Supplementary material

Supplementary data to this article can be found online at https://doi.org/10.1016/j.precamres.2022.106738.

References

Belousova, E.A., Griffin, W.L., O'Reilly, S.Y., Fisher, N.I., 2002. Igneous zircon: Trace element composition as an indicator of source rock type. Contrib. Miner. Petrol. 143 (5), 602–622.
Berry, R.F., Jenner, G.A., Meffre, S., Tubrett, M.N., 2001. A North American provenance for Neoproterozoic to Cambrian sandstones in Tasmania? Earth Planet. Sci. Lett. 192 (2), 207–222.
Bgmrsp, 1991. Bureau of Geology and Mineral Resources of Sichuan Province. In: Regional Geology of the Sichuan Province. Geological Publishing House, Beijing, pp. 1–730 in Chinese.
Blichert-Toft, J., Albarède, F., 1997. The Lu-Hf geochemistry of chondrites and evolution of chondrites and evolution of the mantle-crust system. Earth Planet. Sci. Lett. 148 (1–2), 243–258.
Boger, S.D., Wilson, C.J.L., Fanning, C.M., 2001. Early Paleozoic tectonism within the East Antarctic craton: The final suture between east and west Gondwana? Geology 29 (5), 463–466.
Bruguier, O., Lancelot, J.R., Malavieille, J., 1997. U-Pb dating on single detrital zircon grains from the Triassic Songpan-Ganze flysch (Central China): Provenance and tectonic correlations. Earth Planet. Sci. Lett. 152 (1), 217–231.
Burchfiel, B.C., Chen, Z.L., Liu, Y.P., Royden, L.H., 1995. Tectonics of the Longmen Shan and adjacent regions, central China. Int. Geol. Rev. 37 (8), 661–735.
Burchfiel, B.C., Chen, Z.L., 2012. Tectonics of the southeastern Tibetan Plateau and its adjacent foreland. Geological Society of America, Colorado, United States, pp. 1–164.
Burrett, C., Khin, Z., Meffre, S., Lai, C.K., Khositanont, S., Chaodumrong, P., 2014. The configuration of Greater Gondwana—Evidence from LA ICPMS, U-Pb geochronology of detrital zircons from the Palaeozoic and Mesozoic of Southeast Asia and China. Gondwana Res. 26 (1), 31–51.
Cawood, P.A., Johnson, M.R., Nemchin, A.A., 2007. Early Palaeozoic orogenesis along the Indian margin of Gondwana: Tectonic response to Gondwana assembly. Earth Planet. Sci. Lett. 255 (1–2), 70–84.
Cawood, P.A., Nemchin, A.A., 2000. Provenance record of a rift basin: U/Pb ages of detrital zircons from the Perth Basin. Western Australia. Sed. Geol. 134 (3–4), 209–234.
Cawood, P.A., Wang, Y.J., Xu, Y.J., Zhao, G.C., 2013. Locating South China in Rodinia and Gondwana: A fragment of greater India lithosphere? Geology 41 (8), 903–906.
Chang, E.Z., 2000. Geology and tectonics of the Songpan-Ganzi fold belt, southwestern China. Int. Geol. Rev. 42 (9), 813–831.
Chen, F.L., Cui, X.Z., Lin, S.F., Wang, J., Yang, X.M., Ren, G.M., Pang, W.H., 2021a. The 1.14 Ga mafic intrusions in the SW Yangtze Block, South China: Records of late Mesoproterozoic intraplate magmatism. J. Asian Earth Sci. 205, 104603.
Chen, J.L., Xu, J.F., Ren, J.B., Huang, X.X., Wang, B.D., 2014a. Geochronology and geochemical characteristics of Late Triassic porphyritic rocks from the Zhongdian arc, eastern Tibet, and their tectonic and metallogenic implications. Gondwana Res. 26 (2), 492–504.
Chen, Q., Sun, M., Long, X., Yuan, C., 2015. Petrogenesis of Neoproterozoic adakitic tonalites and high-K granites in the eastern Songpan-Ganze Fold Belt and implications for the tectonic evolution of the western Yangtze Block. Precambr. Res. 270, 181–203.
Chen, Q., Sun, M., Long, X., Zhao, G., Wang, J., Yu, Y., Yuan, C., 2018a. Provenance study for the Paleozoic sedimentary rocks from the west Yangtze Block: Constraint on possible link of South China to the Gondwana supercontinent reconstruction. Precambr. Res. 309, 271–289.
Chen, Q., Sun, M., Long, X.P., Zhao, G.C., Yuan, C., 2016. U-Pb ages and Hf isotopic record of zircons from the late Neoproterozoic and Silurian-Devonian sedimentary rocks of the western Yangtze Block: Implications for its tectonic evolution and continental affinity. Gondwana Res. 31, 184–199.
Chen, Q., Sun, M., Zhao, G.C., Zhao, J.H., Zhu, W.L., Long, X.P., Wang, J., 2019. Episodic crustal growth and reworking of the Yudongzi terrane, South China: Constraints from the Archean TTGs and potassic granites and Paleoproterozoic amphibolites. Lithos 326–327, 1–18.
Chen, Q., Zhao, G.C., Sun, M., 2021b. Protracted northward drifting of South China during the assembly of Gondwana: Constraints from the spatial-temporal provenance comparison of Neoproterozoic−Cambrian strata. Geol. Soc. Am. Bull. 133 (9-10): 1947–1963.
Chen, W.T., Sun, W.H., Wang, W., Zhao, J.H., Zhou, M.F., 2014b. "Grenvillian" intra-plate mafic magmatism in the southwestern Yangtze Block, SW China. Precambr. Res. 242, 138–153.
Chen, W.T., Sun, W.H., Zhou, M.F., Wang, W., 2018b. Ca. 1050 Ma intra-continental rift-related A-type felsic rocks in the southwestern Yangtze Block. South China. Precambr. Res. 309, 22–44.
Chen, W.T., Zhou, M.F., Zhao, X.F., 2013. Late Paleoproterozoic sedimentary and mafic rocks in the Hekou area, SW China: Implication for the reconstruction of the Yangtze Block in Columbia. Precambr. Res. 231 (5), 61–77.

Chen, Y.X., Pei, X.Z., Li, R.B., Li, Z.C., Pei, L., Liu, C.J., Yang, J., 2014c. Geochemical characteristics and tectonic significance of meta-sedimentary rocks from NaiJ Tal Group, eastern section of East Kunlun. Geoscience 28 (03), 489–500 in Chinese with English abstract.
Corfu, F., Hanchar, J.M., Hoskin, P.W.O., Kinny, P., 2003. Atlas of zircon textures. Rev. Mineral. Geochem. 53 (1), 469–500.
Cui, X.Z., Wang, J., Ren, G.M., Deng, Q., Sun, Z.M., Ren, F., Chen, F.L., 2020. Paleoproterozoic tectonic evolution of the Yangtze Block: New evidence from ca. 2.36 to 2.22 Ga magmatism and 1.96 Ga metamorphism in the Cuoke complex, SW China. Precambr. Res. 337, 105525.
Ding, L., Yang, D., Cai, F.L., Pullen, A., Kapp, P., Gehrels, G.E., Zhang, L.Y., Zhang, Q.H., Lai, Q.Z., Yue, Y.H., Shi, R.D., 2013. Provenance analysis of the Mesozoic Hoh-Xil-Songpan-Ganzi turbidites in northern Tibet: Implications for the tectonic evolution of the eastern Paleo-Tethys Ocean. Tectonics 32 (1), 34–48.
Dong, C.Y., Li, C., Wan, Y.S., Wang, W., Wu, Y.W., Xie, H.Q., Liu, D.Y., 2011. Detrital zircon age mode of Ordovician Wenquan quartzite south of Lungmuco-Shuanghu Suture in the Qiangtang area, Tibet: Constraint on tectonic affinity and source regions. Sci. China Earth Sci. 54 (7), 1034–1042.
Dong, X., Zhang, Z.M., Wang, G.L., Zhao, G.C., Liu, F., Wang, W., Yu, F., 2009. Provencance and formation age of the Nyingchi Group in the southern Lhasa Terrane, Tibetan Plateau: Petrology and zircon U-Pb geochronology. Acta Petrol. Sin. 25 (07), 1678–1694 in Chinese with English abstract.
Dong, Y.P., He, D.F., Sun, S.S., Liu, X.M., Zhou, X.H., Zhang, F.F., Yang, Z., Cheng, B., Zhao, G.C., Li, J.H., 2018. Subduction and accretionary tectonics of the East Kunlun orogen, western segment of the Central China Orogenic System. Earth Sci. Rev. 186, 231–261.
Du, Q.L., 1986. The discovery and subdivision of Precambrian in Shuiluo area, Muli Country. Sichuan Province. J. Chengdu Coll. Geol. 13 (1), 31–49 in Chinese with English abstract.
Duan, L., Meng, Q.R., Zhang, C.L., Liu, X.M., 2011. Tracing the position of the South China block in Gondwana: U-Pb ages and Hf isotopes of Devonian detrital zircons. Gondwana Res. 19 (1), 141–149.
Duan, L., Meng, Q.R., Wu, G.L., Ma, S.X., Li, L., 2012. Detrital zircon evidence for the linkage of the South China block with Gondwanaland in early Palaeozoic time. Geol. Mag. 149 (6), 1124–1131.
Enkelmann, E., Weislogel, A., Ratschbacher, L., Eide, E., Renno, A., Wooden, J., 2007. How was the Triassic Songpan-Ganzi basin filled? A provenance study. Tectonics 26 (4).
Fedo, C.M., Sircombe, C.M., Rainbird, R.H., 2003. Detrital Zircon Analysis of the Sedimentary Record. Rev. Mineral. Geochem. 53, 277–303.
Fergusson, C.L., Carr, P.F., Fanning, C.M., Green, T.J., 2001. Proterozoic-Cambrian detrital zircon and monazite ages from the Anakie Inlier, central Queensland: Grenville and Pacific-Gondwana signatures. Aust. J. Earth Sci. 48 (6), 857–866.
Fitzsimons, I.C.W., 2000. Grenville-age basement provinces in East Antarctica: Evidence for three separate collisional orogens. Geology 28 (10), 879–882.
Gao, S., Yang, J., Zhou, L., Li, M., Hu, Z.C., Guo, J.L., Xiao, G.Q., Wei, J.Q., 2011. Age and growth of the Archean Kongling terrain, South China, with emphasis on 3.3 Ga granitoid gneisses. Am. J. Sci. 311 (2), 153–182.
Gao, X., Yang, L.Q., Meng, J.Y., Zhang, L.J., 2017. Zircon U-Pb, molybdenite Re–Os geochronology and Sr–Nd–Pb–Hf–O–S isotopic constraints on the genesis of Relin Cu–Mo deposit in Zhongdian, Northwest Yunnan. China. Ore Geol. Rev. 91, 945–962.
Gehrels, G., 2012. Detrital zircon U-Pb geochronology: Current methods and new opportunities. In: Tectonics of sedimentary basins: Recent Advances. Blackwell Publishing Ltd, Oxford, pp. 45–62.
Gehrels, G., Kapp, P., DeCelles, P., Pullen, A., Blakey, R., Weislogel, A., Ding, L., Guynn, J., Martin, A., McQuarrie, N., Yin, A., 2011. Detrital zircon geochronology of pre-Tertiary strata in the Tibetan-Himalayan orogen. Tectonics 30 (5).
Gehrels, G.E., DeCelles, P.G., Ojha, T.P., Upreti, B.N., 2006a. Geologic and U-Th-Pb geochronologic evidence for early Paleozoic tectonism in the Kathmandu thrust sheet, central Nepal Himalaya. Geol. Soc. Am. Bull. 118 (1–2), 185–198.
Gehrels, G.E., DeCelles, P.G., Ojha, T.P., Upreti, B.N., 2006b. Geologic and U-Pb geochronologic evidence for early Paleozoic tectonism in the Dadeldhura thrust sheet, far-west Nepal Himalaya. J. Asian Earth Sci. 28 (4–6), 385–408.
Gong, R.X., Yan, T.Z., Yu, X.Q., Hua, X.H., Zhang, Z.F., 2009. Subdivision and geological age of Pingshui Group in Zhejiang. China. Geoscience 23 (02), 238–245 in Chinese with English abstract.
Goodge, J.W., Myrow, P., Williams, I.S., Bowring, S.A., 2002. Age and provenance of the Beardmore Group, Antarctica: Constraints on Rodinia supercontinent breakup. J. Geol. 110 (4), 393–406.
Greentree, M.R., Li, Z.X., 2008. The oldest known rocks in south–western China: SHRIMP U-Pb magmatic crystallisation age and detrital provenance analysis of the Paleoproterozoic Dahongshan Group. J. Asian Earth Sci. 33 (5–6), 289–302.
Grew, E.S., Carson, C.J., Christy, A.G., Maas, R., Yaxley, G.M., Boger, S.D., Fanning, C.M., 2012. New constraints from U-Pb, Lu–Hf and Sm–Nd isotopic data on the timing of sedimentation and felsic magmatism in the Larsemann Hills, Prydz Bay, East Antarctica. Precambr. Res. 206–207, 87–108.
Griffin, W.L., Belousova, E.A., Shee, S.R., Pearson, N.J., O'Reilly, S.Y., 2004. Archean crustal evolution in the northern Yilgarn Craton: U-Pb and Hf-isotope evidence from detrital zircons. Precambr. Res. 131 (3–4), 231–282.
Griffin, W.L., Pearson, N.J., Belousova, E., Jackson, S.E., van Achterbergh, E., O'Reilly, S. Y., Shee, S.R., 2000. The Hf isotope composition of cratonic mantle: LAM-MC-ICPMS analysis of zircon megacrysts in kimberlites. Geochim. Cosmochim. Acta 64 (1), 133–147.
Grimes, C.B., John, B.E., Kelemen, P.B., Mazdab, F.K., Wooden, J.L., Cheadle, M.J., Hanghøj, K., Schwartz, J.J., 2007. Trace element chemistry of zircons from oceanic crust: A method for distinguishing detrital zircon provenance. Geology 35 (7), 643–646.
Guo, J.H., Leng, C.B., Zhang, X.C., Zafar, T., Chen, W.T., Zhang, W., Tian, Z.D., Tian, F., Lai, C.K., 2020. Textural and chemical variations of magnetite from porphyry Cu-Au and Cu skarn deposits in the Zhongdian region, northwestern Yunnan. SW China. Ore Geol. Rev. 116, 103245.
Halpin, J.A., Daczko, N.R., Clarke, G.L., Murray, K.R., 2013. Basin analysis in polymetamorphic terranes: An example from east Antarctica. Precambr. Res. 231, 78–97.
Hanchar, J.M., Rudnick, R.L., 1995. Revealing hidden structures: The application of cathodoluminescence and back-scattered electron imaging to dating zircons from lower crustal xenoliths. Lithos 36 (3–4), 289–303.
Hoffman, P.F., 1991. Did the breakout of laurentia turn gondwanaland inside-out? Science 252 (5011), 1409–1412.
Hofmann, M., Linnemann, U., Rai, V., Becker, S., Gärtner, A., Sagawe, A., 2011. The India and South China cratons at the margin of Rodinia—Synchronous Neoproterozoic magmatism revealed by LA-ICP-MS zircon analyses. Lithos 123 (1–4), 176–187.
Hoskin, P.W.O., Ireland, T.R., 2000. Rare earth element chemistry of zircon and its use as a provenance indicator. Geology 28 (7), 627–630.
Hoskin, P.W.O., Schaltegger, U., 2003. The composition of zircon and igneous and metamorphic petrogenesis. Rev. Mineral. Geochem. 53 (1), 27–62.
Hou, Z.Q., Khin, Z., Qu, X.M., Ye, Q.T., Yu, J.J., Xu, M.J., Fu, D.M., Yin, X.K., 2001. Origin of the Gacun volcanic-hosted massive sulfide deposit in Sichuan, China: Fluid inclusion and oxygen isotope evidence. Econ. Geol. 96 (7), 1491–1512.
Hou, Z.Q., Yang, Y.Q., Wang, H.P., Qu, X.M., Lv, Q.T., Huang, D.H., Wu, X.Z., Yu, J.J., Tang, S.H., Zhao, J.H., 2003. Collision-Orogenic Processes and Mineralization Systems of the Yidun arc. Geological Publishing House, Beijing, pp. 1–345 in Chiese with English abstract.
Hu, J., Liu, X.C., Chen, L.Y., Qu, W., Li, H.K., Geng, J.Z., 2013. A ~2.5 Ga magmatic event at the northern margin of the Yangtze craton: Evidence from U-Pb dating and Hf isotope analysis of zircons from the Douling Complex in the South Qinling orogen. Chin. Sci. Bull. 58 (28–29), 3564–3579.
Hu, P.Y., Zhai, Q.G., Zhao, G.C., Wang, J., Tang, Y., Zhu, Z.C., Wu, H., 2019. The North Lhasa terrane in Tibet was attached with the Gondwana before it was drafted away in Jurassic: Evidence from detrital zircon studies. J. Asian Earth Sci. 185, 104055.
Hu, Z.C., Liu, Y.S., Gao, S., Liu, W.G., Zhang, W., Tong, X.R., Lin, L., Zong, K.Q., Li, M., Chen, H.H., Zhou, L., Yang, L., 2012. Improved in situ Hf isotope ratio analysis of zircon using newly designed X skimmer cone and jet sample cone in combination with the addition of nitrogen by laser ablation multiple collector ICP-MS. J. Anal. At. Spectrom. 27, 1391–1399.
Huang, D.L., Wang, X.L., 2019. Reviews of geochronology, geochemistry, and geodynamic processes of Ordovician-Devonian granitic rocks in southeast China. J. Asian Earth Sci. 184, 104001.
Huang, X.L., Xu, Y.G., Lan, J.B., Yang, Q.J., Luo, Z.Y., 2009. Neoproterozoic adakitic rocks from Mopanshan in the western Yangtze Craton: Partial melts of a thickened lower crust. Lithos 112 (3), 367–381.
Huang, X.L., Xu, Y.G., Li, X.H., Li, W.X., Lan, J.B., Zhang, H.H., Liu, Y.S., Wang, Y.B., Li, H.Y., Luo, Z.Y., Yang, Q.J., 2008. Petrogenesis and tectonic implications of Neoproterozoic, highly fractionated A-type granites from Mianning. South China. Precambr. Res. 165 (3), 190–204.
Huang, X.X., Xu, J.F., Chen, J.L., Ren, J.B., 2012. Geochronology, geochemistry and petrogegesis of two periods of intermediate-acid intrusive rocks from Hongshan area in Zhongdian arc. Acta Petrol. Sin. 28 (5), 1493–1506 in Chinese with English abstract.
Hughes, N.C., Myrow, P.M., McKenzie, N.R., Harper, D.A.T., Bhargava, O.N., Tangri, S. K., Ghalley, K.S., Fanning, C.M., 2011. Cambrian rocks and faunas of the Wachi La, Black Mountains. Bhutan. Geol. Mag. 148 (3), 351–379.
Ireland, T.R., Flöttmann, T., Fanning, C.M., Gibson, G.M., Preiss, W.V., 1998. Development of the early Paleozoic Pacific margin of Gondwana from detrital-zircon ages across the Delamerian orogen. Geology 26(3), 243-246.
Jackson, W.T., Robinson, D.M., Weislogel, A.L., Jian, X., 2020. Cenozoic reactivation along the Late Triassic Ganzi-Litang suture, eastern Tibetan Plateau. Geosci. Front. 11 (3), 1069–1080.
Jian, P., Liu, D.Y., Kröner, A., Zhang, Q., Wang, Y.Z., Sun, X.M., Zhang, W., 2009. Devonian to Permian plate tectonic cycle of the Paleo-Tethys Orogen in southwest China (II): Insights from zircon ages of ophiolites, arc/back-arc assemblages and within-plate igneous rocks and generation of the Emeishan CFB province. Lithos 113 (3–4), 767–784.
Jin, L.J., Zhou, H.W., Wang, J.L., Zhu, Y.H., Lin, Q.X., 2015. LA-ICP-MS U-Pb dating of the detrital zircons from clastic rocks of Naij Tal Group in East Kunlun and its geological implications. Geol. Bull. China 34 (10), 1848–1859 in Chinese with English abstract.
Lai, C.K., Meffre, S., Crawford, A.J., Zaw, K., Halpin, J.A., Xue, C.D., Salam, A., 2014a. The Central Ailaoshan ophiolite and modern analogs. Gondwana Res. 26 (1), 75–88.
Lai, C.K., Meffre, S., Crawford, A.J., Zaw, K., Xue, C.D., Halpin, J.A., 2014b. The Western Ailaoshan Volcanic Belts and their SE Asia connection: A new tectonic model for the Eastern Indochina Block. Gondwana Res. 26 (1), 52–74.
Leng, C.B., Gao, J.F., Chen, W.T., Zhang, X.C., Tian, Z.D., Guo, J.H., 2018. Platinum-group elements, zircon Hf-O isotopes, and mineralogical constraints on magmatic evolution of the Pulang porphyry Cu-Au system. SW China. Gondwana Res. 62, 163–177.
Leng, C.B., Huang, Q.Y., Zhang, X.C., Wang, S.X., Zhong, H., Hu, R.Z., Bi, X.W., Zhu, J.J., Wang, X.S., 2014. Petrogenesis of the Late Triassic volcanic rocks in the Southern Yidun arc, SW China: Constraints from the geochronology, geochemistry, and Sr–Nd–Pb–Hf isotopes. Lithos 190–191, 363–382.

Leng, C.B., Zhang, X.C., Hu, R.Z., Wang, S.X., Zhong, H., Wang, W.Q., Bi, X.W., 2012. Zircon U-Pb and molybdenite Re–Os geochronology and Sr–Nd–Pb–Hf isotopic constraints on the genesis of the Xuejiping porphyry copper deposit in Zhongdian, Northwest Yunnan. China. J. Asian Earth Sci. 60 (22), 31–48.
Li, J.Y., Wang, X.L., Gu, Z.D., 2018. Early Neoproterozoic arc magmatism of the Tongmuliang Group on the northwestern margin of the Yangtze Block: Implications for Rodinia assembly. Precambr. Res. 309, 181–197.
Li, L.M., Lin, S.F., Xing, G.F., Davis, D.W., Davis, W.J., Xiao, W.J., Yin, C.Q., 2013a. Geochemistry and tectonic implications of late Mesoproterozoic alkaline bimodal volcanic rocks from the Tieshajie Group in the southeastern Yangtze Block, South China. Precambr. Res. 230, 179–192.
Li, Q.H., Zhang, Y.X., Zhang, K.J., Yan, L.L., Zeng, L., Jin, X., Sun, J.F., Zhou, X.Y., Tang, X.C., Lu, L., 2017a. Garnet amphibolites from the Ganzi-Litang fault zone, eastern Tibetan Plateau: mineralogy, geochemistry, and implications for evolution of the eastern Palaeo-Tethys Realm. Int. Geol. Rev. 60, 1–14.
Li, W.C., Zeng, P.S., Hou, Z.Q., White, N.C., 2011. The Pulang Porphyry Copper Deposit and Associated Felsic Intrusions in Yunnan Province. Southwest China. Econ. Geol. 106 (1), 79–92.
Li, W.C., Yu, H.J., Gao, X., Liu, X.L., Wang, J.H., 2017b. Review of Mesozoic multiple magmatism and porphyry Cu–Mo (W) mineralization in the Yidun Arc, eastern Tibet Plateau. Ore Geol. Rev. 90, 795–812.
Li, X.H., Li, Z.X., Zhou, H.W., Liu, Y., Kinny, P.D., 2002. U-Pb zircon geochronology, geochemistry and Nd isotopic study of Neoproterozoic bimodal volcanic rocks in the Kangdian Rift of South China: Implications for the initial rifting of Rodinia. Precambr. Res. 113 (1), 135–154.
Li, X.H., Tang, G.Q., Gong, B., Yang, Y.H., Hou, K.J., Hu, Z.C., Li, Q.L., Liu, Y., Li, W.X., 2013b. Qinghu zircon: A working reference for microbeam analysis of U-Pb age and Hf and O isotopes. Chin. Sci. Bull. 58 (36), 4647–4654.
Li, X.Z., Liu, Z.Q., Pan, G.T., Luo, J.N., Wang, Z., Zheng, L.L., 1991. The dividing and evolution of tectonic unit of Sanjiang, Southwest China. Bulletin of the Chengdu institute of geology and mineral resources. Chin. Acad. Geol. Sci. 13, 1–20 in Chinese with English abstract.
Li, Z.X., Evans, D.A.D., Halverson, G.P., 2013c. Neoproterozoic glaciations in a revised global palaeogeography from the breakup of Rodinia to the assembly of Gondwanaland. Sed. Geol. 294, 219–232.
Liu, B.B., Peng, T.P., Fan, W.M., Zhao, G.C., Gao, J.F., Dong, X.H., Peng, B.X., 2020. Tectonic evolution and paleoposition of the Baoshan and Lincang blocks of west Yunnan during the Paleozoic. Tectonics 39 (10).
Liu, H.C., Xia, X.P., Lai, C.K., Gan, C.S., Zhou, Y.Z., Huangfu, P.P., 2018. Break-away of South China from Gondwana: Insights from the Silurian high-Nb basalts and associated magmatic rocks in the Diancangshan-Ailaoshan fold belt (SW China). Lithos 318–319, 194–208.
Liu, X.M., Gao, S., Diwu, C.R., Ling, W.L., 2008a. Precambrian crustal growth of Yangtze Craton as revealed by detrital zircon studies. Am. J. Sci. 308 (4), 421–468.
Liu, Y.S., Gao, S., Hu, Z.C., Gao, C.G., Zong, K.Q., Wang, D.B., 2010. Continental and oceanic crust recycling-induced melt–peridotite interactions in the Trans-North China Orogen: U-Pb dating, Hf isotopes and trace elements in zircons from mantle xenoliths. J. Petrol. 51 (1–2), 537–571.
Liu, Y.J., Genser, J., Neubauer, F., Jin, W., Ge, X.H., Handler, R., Takasu, A., 2005. $^{40}Ar/^{39}Ar$ mineral ages from basement rocks in the Eastern Kunlun Mountains, NW China, and their tectonic implications. Tectonophysics 398 (3–4), 199–224.
Liu, Y.S., Hu, Z.C., Gao, S., Gunther, D., Xu, J., Gao, C.G., Chen, H.H., 2008b. In situ analysis of major and trace elements of anhydrous minerals by LA-ICP-MS without applying an internal standard. Chem. Geol. 257 (1–2), 34–43.
Long, S., McQuarrie, N., Tobgay, T., Rose, C., Gehrels, G., Grujic, D., 2011. Tectonostratigraphy of the Lesser Himalaya of Bhutan: Implications for the along-strike stratigraphic continuity of the northern Indian margin. Geol. Soc. Am. Bull. 123 (7–8), 1406–1426.
Long, X.P., Luo, J., Sun, M., Wang, X.C., Wang, Y.J., Yuan, C., Jiang, Y.D., 2020. Detrital zircon U-Pb ages and whole-rock geochemistry of early Paleozoic metasedimentary rocks in the Mongolian Altai: Insights into the tectonic affinity of the whole Altai-Mongolian terrane. Geol. Soc. Am. Bull. 132 (3–4), 477–494.
Long, X.P., Yuan, C., Sun, M., Xiao, W.J., Zhao, G.C., Wang, Y.J., Cai, K.D., Xia, X.P., Xie, L.W., 2010. Detrital zircon U-Pb ages and Hf isotopes of the early Paleozoic flysch sequence in the Chinese Altai, NW China: New constrains on depositional age, provenance and tectonic evolution. Tectonophysics 480, 213–231.
Lu, G.M., Wang, W., Tian, Y., Spencer, C.J., Huang, S.F., Xue, E.K., Huang, B., 2021. Siderian mafic-intermediate magmatism in the SW Yangtze Block, South China: Implications for global 'tectono-magmatic lull'during the early Paleoproterozoic. Lithos 398.
Ludwig, K.R., 2003. User's Manual for isoplot 3.00, a geochronological toolkit for Microsoft Excel. Berkeley Geochronology Center Special Publication, Berkeley, pp. 25-32.
Luo, A.B., Fan, J.J., Hao, Y.J., Li, H., Zhang, B.C., 2020. Aptian flysch in central Tibet: Constraints on the timing of closure of the Bangong-Nujiang Tethyan Ocean. Tectonics 39(12), e2020TC006198.
Luo, B.J., Liu, R., Zhang, H.F., Zhao, J.H., Yang, H., Xu, W.C., Guo, L., Zhang, L.Q., Tao, L., Pan, F.B., Wang, W., Gao, Z., Shao, H., 2018. Neoproterozoic continental back-arc rift development in the Northwestern Yangtze Block: Evidence from the Hannan intrusive magmatism. Gondwana Res. 59, 27–42.
Lv, Z.H., Chen, J., Zhang, H., Tang, Y., 2021. Petrogenesis of Neoproterozoic rare metal granite-pegmatite suite in Jiangnan Orogen and its implications for rare metal mineralization of peraluminous rock in South China. Ore Geol. Rev. 128, 103923.
Ma, A.L., Hu, X.M., Garzanti, E., Han, Z., Lai, W., 2017. Sedimentary and tectonic evolution of the southern Qiangtang basin: Implications for the Lhasa-Qiangtang collision timing. J. Geophys. Res. 122 (7), 4790–4813.
Ma, Y.M., Wang, Q., Wang, J., Yang, T.S., Tan, X.D., Dan, W., Zhang, X.Z., Ma, L., Wang, Z.L., Hu, W.L., Zhang, S.H., Wu, H.C., Li, H.Y., Cao, L.W., 2019. Paleomagnetic constraints on the origin and drift history of the north Qiangtang Terrane in the late Paleozoic. Geophys. Res. Lett 46 (2), 689–697.
Ma, Y.M., Yang, T.S., Bian, W.W., Jin, J.J., Wang, Q., Zhang, S.H., Wu, H.C., Li, H.Y., Cao, L.W., 2018. A stable southern margin of Asia during the Cretaceous: Paleomagnetic constraints on the Lhasa-Qiangtang collision and the maximum width of the Neo-Tethys. Tectonics 37 (10), 3853–3876.
Markwitz, V., Kirkland, C.L., Wyrwoll, K.H., Hancock, E.A., Evans, N.J., Lu, Y., 2017. Variations in zircon provenance constrain age and geometry of an early Paleozoic rift in the Pinjarra orogen. East Gondwana. Tectonics 36 (11), 2477–2496.
McQuarrie, N., Long, S.P., Tobgay, T., Nesbit, J.N., Gehrels, G., Ducea, M.N., 2013. Documenting basin scale, geometry and provenance through detrital geochemical data: Lessons from the Neoproterozoic to Ordovician Lesser, Greater, and Tethyan Himalayan strata of Bhutan. Gondwana Res. 23 (4), 1491–1510.
McQuarrie, N., Robinson, D., Long, S., Tobgay, T., Grujic, D., Gehrels, G., Ducea, M., 2008. Preliminary stratigraphic and structural architecture of Bhutan: Implications for the along strike architecture of the Himalayan system. Earth Planet. Sci. Lett. 272 (1–2), 105–117.
Meert, J.G., 2003. A synopsis of events related to the assembly of eastern Gondwana. Tectonophysics 362, 1–40.
Meng, E., Liu, F.L., Du, L.L., Liu, P.H., Liu, J.H., 2015. Petrogenesis and tectonic significance of the Baoxing granitic and mafic intrusions, southwestern China: Evidence from zircon U-Pb dating and Lu–Hf isotopes, and whole-rock geochemistry. Gondwana Res. 28 (2), 800–815.
Meng, F.C., Zhang, J.X., Cui, M.H., 2013. Discovery of early Paleozoic eclogite from the East Kunlun, Western China and its tectonic significance. Gondwana Res. 23 (2), 825–836.
Metcalfe, I., 2013. Gondwana dispersion and Asian accretion: Tectonic and palaeogeographic evolution of eastern Tethys. J. Asian Earth Sci. 66, 1–33.
Metcalfe, I., 2021. Multiple Tethyan ocean basins and orogenic belts in Asia. Gondwana Res. 100, 87–130.
Myrow, P., Hughes, N.C., Searle, M., Fanning, C., Peng, S.C., Parcha, S.K., 2009. Stratigraphic correlation of Cambrian-Ordovician deposits along the Himalaya: implications for the age and nature of rocks in the Mount Everest region. Geol. Soc. Am. Bull. 120 (3–4), 323–332.
Myrow, P.M., Hughes, N.C., Goodge, J.W., Fanning, C.M., Williams, I.S., Peng, S.C., Bhargava, O.N., Parcha, S.K., Pogue, K.R., 2010. Extraordinary transport and mixing of sediment across Himalayan central Gondwana during the Cambrian-Ordovician. Geol. Soc. Am. Bull. 122 (9–10), 1660–1670.
Nie, S.Y., Yin, A., Rowley, D.B., Jin, Y.G., 1994. Exhumation of the Dabie Shan ultra-high-pressure rocks and accumulation of the Songpan-Ganzi flysch sequence, central China. Geology 22 (11), 999–1002.
Pan, G.T., Wang, L.Q., Li, R.S., Yuan, S.H., Ji, W.H., Yin, F.G., Zhang, W.P., Wang, B.D., 2012. Tectonic evolution of the Qinghai-Tibet Plateau. J. Asian Earth Sci. 53, 3–14.
Peng, H.J., Mao, J.W., Pei, R.F., Zhang, C.Q., Tian, G., Zhou, Y.M., Li, J.X., Hou, L., 2014. Geochronology of the Hongniu-Hongshan porphyry and skarn Cu deposit, northwestern Yunnan province, China: Implications for mineralization of the Zhongdian arc. J. Asian Earth Sci. 79, 682–695.
Peng, M., Wu, Y.B., Wang, J., Jiao, W.F., Liu, X.C., Yang, S.H., 2009. Paleoproterozoic mafic dyke from Kongling terrain in the Yangtze Craton and its implication. Sci. Bull. 54 (6), 1098–1104.
Peng, M., Wu, Y.B., Gao, S., Zhang, H.F., Wang, J., Liu, X.C., Gong, H.J., Zhou, L., Hu, Z. C., Liu, Y.S., Yuan, H.L., 2012. Geochemistry, zircon U-Pb age and Hf isotope compositions of Paleoproterozoic aluminous A-type granites from the Kongling terrain, Yangtze Block: Constraints on petrogenesis and geologic implications. Gondwana Res. 22 (1), 140–151.
Peng, S.Z., Pei, X.Z., Li, R.B., Li, Z.C., Liu, C.J., Chen, Y.X., Yan, Q.Z., Wang, X., Zhang, Y., Hu, C.G., 2017. Detrital zircon U-Pb age and geological significance of the meta-sedimentary rocks from the Qingshuiquan area in the central tectonic melange belt of East Kunlun. Northwest. Geol. 50 (01), 212–226 in Chinese with English abstract.
Pullen, A., Kapp, P., Gehrels, G.E., Vervoort, J.D., Ding, L., 2008. Triassic continental subduction in central Tibet and Mediterranean-style closure of the Paleo-Tethys Ocean. Geology 36 (5), 351–354.
Qu, X.M., Hou, Z.Q., 2002. ^{40}Ar-^{39}Ar age of the Panyong pillow basalt: Implication for the evolution relationship between the Jinshajiang and Ganze-Litang suture zones. Geol. Rev. 48 (S1), 115–121 in Chinese with English abstract.
Reid, A.J., Wilson, C.J.L., Liu, S., 2005a. Structural evidence for the Permo-Triassic tectonic evolution of the Yidun Arc, eastern Tibetan Plateau. J. Struct. Geol. 27 (1), 119–137.
Reid, A.J., Wilson, C.J.L., Phillips, D., Liu, S., 2005b. Mesozoic cooling across the Yidun Arc, central-eastern Tibetan Plateau: A reconnaissance $^{40}Ar/^{39}Ar$ study. Tectonophysics 398 (1–2), 45–66.
Roger, F., Malavieille, J., Leloup, P.H., Calassou, S., Xu, Z., 2004. Timing of granite emplacement and cooling in the Songpan-Garzê Fold Belt (eastern Tibetan Plateau) with tectonic implications. J. Asian Earth Sci. 22 (5), 465–481.
Scherer, E., Munker, C., Mezger, K., 2001. Calibration of the lutetium-hafnium clock. Science 293 (5530), 683–687.
She, Z.B., Ma, C.Q., Mason, R., Li, J.W., Wang, G.C., Lei, Y.H., 2006. Provenance of the Triassic Songpan-Ganzi flysch, west China. Chem. Geol. 231, 159–175.
Sláma, J., Košler, J., Condon, D.J., Crowley, J.L., Gerdes, A., Hanchar, J.M., Horstwood, M.S.A., Morris, G.A., Nasdala, L., Norberg, N., Schaltegger, U., Schoene, B., Tubrett, M.N., Whitehouse, M.J., 2008. Plešovice zircon — A new natural reference material for U-Pb and Hf isotopic microanalysis. Chem. Geol. 249 (1–2), 1–35.

Song, P.P., Ding, L., Li, Z.Y., Lippert, P.C., Yang, T.S., Zhao, X.X., Fu, J.J., Yue, Y.H., 2015. Late Triassic paleolatitude of the Qiangtang block: Implications for the closure of the Paleo-Tethys Ocean. Earth Planet. Sci. Lett. 424, 69–83.
Song, S.G., Niu, Y.L., Su, L., Xia, X.H., 2013. Tectonics of the North Qilian orogen. NW China. Gondwana Res. 23 (4), 1378–1401.
Song, X.Y., Zhou, M.F., Cao, Z.M., Robinson, P.T., 2004. Late Permian rifting of the South China Craton caused by the Emeishan mantle plume? J. Geol. Soc. London. 161 (5), 773–781.
Spencer, C.J., Harris, R.A., Dorais, M.J., 2012. Depositional provenance of the Himalayan metamorphic core of Garhwal region, India: Constrained by U-Pb and Hf isotopes in zircons. Gondwana Res. 22 (1), 26–35.
Su, B.R., Cui, X.Z., Tian, J.C., Lai, C.K., Ren, F., Ren, G.M., Liu, S.L., 2019. Detrital zircon provenance and palaeogeographic implications of the Ediacaran Shigu Group in the Zhongza Terrane. SW China. Int. Geol. Rev. 62 (17), 2105–2124.
Sun, S.S., McDonough, W.F., 1989. Chemical and isotopic systematics of oceanic basalts: implications for mantle composition and processes. Geol. Soc. London Spec. Publ. 42 (1), 313–345.
Sun, W.H., Zhou, M.F., Gao, J.F., Yang, Y.H., Zhao, X.F., Zhao, J.H., 2009. Detrital zircon U-Pb geochronological and Lu–Hf isotopic constraints on the Precambrian magmatic and crustal evolution of the western Yangtze Block. SW China. Precambr. Res. 172 (1–2), 99–126.
Tian, Z.D., Leng, C.B., Zhang, X.C., Zhou, L.M., Tang, Y.W., 2019a. Recognition of late Triassic Cu-Mo mineralization in the northern Yidun Arc (S.E. Tibetan Plateau): Implications for regional exploration. Minerals 9 (12), 765.
Tian, Z., D., Leng, C.B., Zhang, X.C., Yin, C.J., Zhang, W., Guo, J.H., Tian, F., 2018a. Mineralogical characteristics of chlorites from Precambrian metamorphic rocks in Yidun magmatic arc of Qinghai-Tibet Plateau and their geological implications. J. Earth Sci. Env. 40(1), 36-48. (in Chinese with English abstract).
Tian, Z.D., 2020. Geochemical characteristics and tectonic affinity of the Neoproterozoic to early Paleozoic clastic sedimentary rocks in the Yidun arc. In: Dissertation for the Doctor Degree. Institute of Geochemistry, Chinese Academy of Sciences, pp. 1–234 in Chinese with English abstract.
Tian, Z.D., Leng, C.B., Zhang, X.C., Yin, C.J., Zhang, W., Guo, J.H., Chen, L.H., 2018b. Mineralogical and petrochemical characteristics of the metamorphic basement of Yidun Terrane and their geological implications. Acta Mineral. Sin. 38 (2), 152–165 in Chinese with English abstract.
Tian, Z.D., Leng, C.B., Zhang, X.C., Zafar, T., Zhang, L.J., Hong, W., Lai, C.K., 2019b. Chemical composition, genesis and exploration implication of garnet from the Hongshan Cu-Mo skarn deposit. SW China. Ore Geol. Rev. 112, 103016.
Turner, C.C., Meert, J.G., Pandit, M.K., Kamenov, G.D., 2014. A detrital zircon U-Pb and Hf isotopic transect across the Son Valley sector of the Vindhyan Basin, India: Implications for basin evolution and paleogeography. Gondwana Res. 26 (1), 348–364.
Veevers, J.J., Saeed, A., Belousova, E.A., Griffin, W.L., 2005. U-Pb ages and source composition by Hf-isotope and trace-element analysis of detrital zircons in Permian sandstone and modern sand from southwestern Australia and a review of the paleogeographical and denudational history of the Yilgarn Craton. Earth Sci. Rev. 68 (3–4), 245–279.
Wang, B.Q., Zhou, M.F., Li, J.W., Yan, D.P., 2011a. Late Triassic porphyritic intrusions and associated volcanic rocks from the Shangri-La region, Yidun terrane, Eastern Tibetan Plateau: adakitic magmatism and porphyry copper mineralization. Lithos 127 (1–2), 24–38.
Wang, M., Dai, C.G., Wang, X.H., Chen, Z.S., Ma, H.Z., 2011b. In-situ zircon geochronology and Hf isotope of muscovite-bearing leucogranites from Fanjingshan, Guizhou Province, and constraints on continental growth of the southern China block. Earth Sci. Front. 18 (05), 213–223 in Chinese with English abstract.
Wang, W., Cawood, P.A., Pandit, M.K., Xia, X., Raveggi, M., Zhao, J., Zheng, J., Qi, L., 2021. Fragmentation of South China from greater India during the Rodinia-Gondwana transition. Geology 49 (2), 228–232.
Wang, W., Cawood, P.A., Pandit, M.K., Zhao, J.H., Zheng, J.P., 2019. No collision between Eastern and Western Gondwana at their northern extent. Geology 47 (4), 308–312.
Wang, W., Cawood, P.A., Zhou, M.F., Zhao, J.H., 2016. Paleoproterozoic magmatic and metamorphic events link Yangtze to northwest Laurentia in the Nuna supercontinent. Earth Planet. Sci. Lett. 433, 269–279.
Wang, W., Zeng, M.F., Zhou, M.F., Zhao, J.H., Zheng, J.P., Lan, Z.F., 2018a. Age, provenance and tectonic setting of Neoproterozoic to early Paleozoic sequences in southeastern South China Block: Constraints on its linkage to western Australia-East Antarctica. Precambr. Res. 309, 290–308.
Wang, W., Zhou, M.F., 2014. Provenance and tectonic setting of the Paleo- to Mesoproterozoic Dongchuan Group in the southwestern Yangtze Block, South China: Implication for the breakup of the supercontinent Columbia. Tectonophysics 610, 110–127.
Wang, X.C., Li, X.H., Li, W.X., Li, Z.X., Liu, Y., Yang, Y., Liang, X.R., Tu, X.L., 2008. The Bikou basalts in the northwestern Yangtze block, South China: Remnants of 820–810 Ma continental flood basalts? Geol. Soc. Am. Bull. 120 (11–12), 1478–1492.
Wang, X.H., Lang, X.H., Tang, J.X., Deng, Y.L., He, Q., Xie, F.W., Li, L., Yin, Q., Li, Z. J., Zhang, L., Yang, Z.Y., Dong, S.Y., Ding, F., Wang, Z.H., Huang, Y., 2020. Early carboniferous back-arc rifting-related magmatism in southern Tibet: Implications for the history of the Lhasa terrane separation from Gondwana. Tectonics 39(10), e2020TC006237.
Wang, X.F., Metcalfe, I., Jian, P., He, L.Q., Wang, C.S., 2000. The Jinshajiang-Ailaoshan Suture Zone, China: Tectonostratigraphy, age and evolution. J. Asian Earth Sci. 18 (6), 675–690.
Wang, X.L., Zhou, J.C., Qiu, J.S., Zhang, W.L., Liu, X.M., Zhang, G.L., 2006. LA-ICP-MS U-Pb zircon geochronology of the Neoproterozoic igneous rocks from Northern Guangxi, South China: Implications for tectonic evolution. Precambr. Res. 145 (1–2), 111–130.
Wang, X.S., Bi, X.W., Leng, C.B., Zhong, H., Tang, H.F., Chen, Y.W., Yin, G.H., Huang, D. Z., Zhou, M.F., 2014a. Geochronology and geochemistry of Late Cretaceous igneous intrusions and Mo–Cu–(W) mineralization in the southern Yidun Arc, SW China: Implications for metallogenesis and geodynamic setting. Ore Geol. Rev. 61, 73–95.
Wang, Y.J., Zhang, A.M., Cawood, P.A., Fan, W.M., Xu, J.F., Zhang, G.W., Zhang, Y.Z., 2013b. Geochronological, geochemical and Nd–Hf–Os isotopic fingerprinting of an early Neoproterozoic arc–back-arc system in South China and its accretionary assembly along the margin of Rodinia. Precambr. Res. 231, 343–371.
Wang, Y.J., Zhang, F.F., Fan, W.M., Zhang, G.W., Chen, S.Y., Cawood, P.A., Zhang, A.M., 2010. Tectonic setting of the South China Block in the early Paleozoic: Resolving intracontinental and ocean closure models from detrital zircon U-Pb geochronology. Tectonics 29 (6).
Wang, Y.J., Zhang, Y.Z., Fan, W.M., Geng, H.Y., Zou, H.P., Bi, X.W., 2014b. Early Neoproterozoic accretionary assemblage in the Cathaysia Block: Geochronological, Lu–Hf isotopic and geochemical evidence from granitoid gneisses. Precambr. Res. 249, 144–161.
Webb, A.A.G., Yin, A., Harrison, T.M., Celerier, J., Gehrels, G.E., Manning, C.E., Grove, M., 2011. Cenozoic tectonic history of the Himachal Himalaya (northwestern India) and its constraints on the formation mechanism of the Himalayan orogen. Geosphere 7 (4), 1013–1061.
Weislogel, A.L., Graham, S.A., Chang, E.Z., Wooden, J.L., Gehrels, G.E., Yang, H., 2006. Detrital zircon provenance of the Late Triassic Songpan-Ganzi complex: Sedimentary record of collision of the North and South China blocks. Geology 34 (2), 97–100.
Wu, T., Xiao, L., Wilde, S.A., Ma, C.Q., Zhou, J.X., 2017. A mixed source for the Late Triassic Garzê-Daocheng granitic belt and its implications for the tectonic evolution of the Yidun arc belt, eastern Tibetan Plateau. Lithos 288–289, 214–230.
Xia, X.P., Nie, X.S., Lai, C.K., Wang, Y.J., Long, X.P., Meffre, S., 2016. Where was the Ailaoshan Ocean and when did it open: A perspective based on detrital zircon U-Pb age and Hf isotope evidence. Gondwana Res. 36, 488–502.
Xia, X.P., Xu, J., Huang, C., Long, X.P., Zhou, M.L., 2020. Subduction polarity of the Ailaoshan Ocean (eastern Paleotethys): Constraints from detrital zircon U-Pb and Hf-O isotopes for the Longtan Formation. Geol. Soc. Am. Bull. 132 (5–6), 987–996.
Xiao, L., Xu, Y.G., Xu, J.F., He, B., Franco, P., 2004. Chemostratigraphy of Flood basalts in the Garzê-Litang region and Zhongza block: implications for western extension of the emeishan large igneous province. SW China. Acta Geol. Sin. 78 (1), 61–67.
Xu, Y.J., Cawood, P.A., Du, Y.S., Hu, L.S., Yu, W.C., Zhu, Y.H., Li, W.C., 2013. Linking south China to northern Australia and India on the margin of Gondwana: Constraints from detrital zircon U-Pb and Hf isotopes in Cambrian strata. Tectonics 32 (6), 1547–1558.
Xue, E.K., Wang, W., Zhou, M.F., Pandit, M.K., Huang, S.F., Lu, G.M., 2021. Late Neoproterozoic–early Paleozoic basin evolution in the Cathaysia Block, South China: Implications of spatio-temporal provenance changes on the paleogeographic reconstructions in supercontinent cycles. Geol. Soc. Am. Bull. 133 (3–4), 717–739.
Yan, D.P., Zhou, M.F., Wei, G.Q., Liu, H., Dong, T.Z., Zhang, W.C., Jin, Z.L., 2008. Collapse of Songpan-Garzê orogenic belt resulted from Mesozoic middle-crustal ductile channel flow: Evidences from deformation and metamorphism within Sinian-Paleozoic strata in hinterland of Longmenshan foreland thrust belt. Earth Sci. Front. 15 (3), 186–198.
Yan, Q.R., Wang, Z.Q., Liu, S.W., Li, Q.G., Zhang, H.Y., Wang, T., Liu, D.Y., Shi, Y.R., Jian, P., Wang, J.G., 2005. Opening of the Tethys in southwest China and its significance to the breakup of East Gondwanaland in late Paleozoic: Evidence from SHRIMP U-Pb zircon analyses for the Garzê ophiolite block. Chin. Sci. Bull. 50 (3), 256–264.
Yan, Q.Z., Pei, X.Z., Li, R.B., Li, Z.C., Pei, L., Liu, C.J., Chen, Y.X., Hu, C.G., Zhang, Y., Wang, X., Peng, S.Z., 2017. Detrital zircon U-Pb age and geological significance of metamorphic strata at Gouli area in the central tectonic belt of East Kunlun. Northwest. Geol. 50 (01), 165–181 in Chinese with English abstract.
Yang, C., Li, X.H., Li, Z.X., Zhu, M., Lu, K., 2020. Provenance evolution of age-calibrated strata reveals when and how South China Block collided with Gondwana. Geophys. Res. Lett. 47 (19).
Yang, L.Q., Gao, X., Shu, Q.H., 2017. Multiple Mesozoic porphyry-skarn Cu (Mo–W) systems in Yidun Terrane, east Tethys: Constraints from zircon U-Pb and molybdenite Re–Os geochronology. Ore Geol. Rev. 90, 813–826.
Yang, T.N., Hou, Z.Q., Wang, Y., Zhang, H.R., Wang, Z.L., 2012. Late Paleozoic to Early Mesozoic tectonic evolution of northeast Tibet: Evidence from the Triassic composite western Jinsha-Garzê-Litang suture. Tectonics 31 (4).
Yang, W.Q., Feng, Q.L., Liu, G.C., 2010. Radiolarian fauna and geochemical characters of the cherts from Garz-Litang tectonic belt and its tectono-Paleogeographic Significance. Acta Geol. Sin. 84 (01), 78–89 in Chinese with English abstract.
Yao, J.L., Shu, L.S., Santosh, M., Zhao, G.C., 2014a. Neoproterozoic arc-related mafic–ultramafic rocks and syn-collision granite from the western segment of the Jiangnan Orogen, South China: Constraints on the Neoproterozoic assembly of the Yangtze and Cathaysia Blocks. Precambr. Res. 243, 39–62.
Yao, W.H., Li, Z.X., Li, W.X., Li, X.H., Yang, J.H., 2014b. From Rodinia to Gondwanaland: A tale of detrital zircon provenance analyses from the southern Nanhua Basin, South China. Am. J. Sci. 314, 278–313.
Yin, A., Harrison, T.M., 2000. Geologic evolution of the Himalayan-Tibetan orogen. Annu. Rev. Earth Planet. Sci. 28 (1), 211–280.
Yu, J.H., Wang, L.J., O'Reilly, S.Y., Griffin, W.L., Zhang, M., Li, C.Z., Shu, L.S., 2009. A Paleoproterozoic orogeny recorded in a long-lived cratonic remnant (Wuyishan terrane), eastern Cathaysia Block. China. Precambr. Res. 174 (3–4), 347–363.
Yuan, H.L., Gao, S., Dai, M.N., Zong, C.L., Günther, D., Fontaine, G.H., Liu, X.M., Diwu, C., 2008. Simultaneous determinations of U-Pb age, Hf isotopes and trace

element compositions of zircon by excimer laser-ablation quadrupole and multiple-collector ICP-MS. Chem. Geol. 247 (1–2), 100–118.
Zhai, Q.G., Li, C., Wang, J., Ji, Z.S., Wang, Y., 2009. SHRIMP U-Pb dating and Hf isotopic analyses of zircons from the mafic dyke swarms in central Qiangtang area. Northern Tibet. Chin. Sci. Bull. 54 (13), 2279–2285.
Zhang, A.M., Wang, Y.J., Fan, W.M., Zhang, Y.Z., Yang, J., 2012a. Earliest Neoproterozoic (ca. 1.0Ga) arc–back-arc basin nature along the northern Yunkai Domain of the Cathaysia Block: Geochronological and geochemical evidence from the metabasite. Precambr. Res. 220–221, 217–233.
Zhang, F.F., Wang, Y.J., Zhang, A.M., Fan, W.M., Zhang, Y.Z., Zi, J.W., 2012b. Geochronological and geochemical constraints on the petrogenesis of Middle Paleozoic (Kwangsian) massive granites in the eastern South China Block. Lithos 150, 188–208.
Zhang, H.F., Parrish, R., Zhang, L., Xu, W.C., Yuan, H.L., Gao, S., Crowley, Q.G., 2007. A-type granite and adakitic magmatism association in Songpan-Garze fold belt, eastern Tibetan Plateau: Implication for lithospheric delamination. Lithos 97 (3), 323–335.
Zhang, H.F., Xu, W.C., Zong, K.Q., Yuan, H.L., Harris, N., 2008. Tectonic evolution of metasediments from the Gangdise terrane, Asian plate, Eastern Himalayan Syntaxis. Tibet. Int. Geol. Rev. 50 (10), 914–930.
Zhang, J.Y., Ma, C.Q., Xiong, F.H., Liu, B., Li, J.W., Pan, Y.M., 2014a. Early Paleozoic high-Mg diorite-granodiorite in the eastern Kunlun Orogen, western China: Response to continental collision and slab break-off. Lithos 210–211, 129–146.
Zhang, K.J., Zhang, Y.X., Tang, X.C., Xia, B., 2012c. Late Mesozoic tectonic evolution and growth of the Tibetan plateau prior to the Indo-Asian collision. Earth Sci. Rev. 114 (3), 236–249.
Zhang, L.Y., Ding, L., Pullen, A., Xu, Q., Liu, D.L., Cai, F.L., Yue, Y.H., Lai, Q.Z., Shi, R.D., Ducea, M.N., Kapp, P., Chapman, A., 2014b. Age and geochemistry of western Hoh-Xil–Songpan-Ganzi granitoids, northern Tibet: Implications for the Mesozoic closure of the Paleo-Tethys ocean. Lithos 190–191, 328–348.
Zhang, S.T., Feng, Q.L., Wang, Y.Z., 2000. Devonian deep-water sediments in Ganze-Litang tectonic belt. Geol. Sci. Tech. Infor. 19 (03), 17–20 in Chinese with English abstract.
Zhang, X.R., Chung, S.L., Lai, Y.M., Ghani, A.A., Murtadha, S., Lee, H.Y., Hsu, C.C., 2018. Detrital Zircons Dismember Sibumasu in East Gondwana. J. Geophys. Res. 123 (7), 6098–6110.
Zhao, G.C., Wang, Y.J., Huang, B.C., Dong, Y.P., Li, S.Z., Zhang, G.W., Yu, S., 2018a. Geological reconstructions of the East Asian blocks: From the breakup of Rodinia to the assembly of Pangea. Earth Sci. Rev. 186, 262–286.
Zhao, J.H., Li, Q.W., Liu, H., Wang, W., 2018b. Neoproterozoic magmatism in the western and northern margins of the Yangtze Block (South China) controlled by slab subduction and subduction-transform-edge-propagator. Earth Sci. Rev. 187, 1–18.
Zhao, J.H., Zhou, M.F., Yan, D.P., Yang, Y.H., Sun, M., 2008a. Zircon Lu–Hf isotopic constraints on Neoproterozoic subduction-related crustal growth along the western margin of the Yangtze Block. South China. Precambr. Res. 163 (3), 189–209.
Zhao, J.H., Zhou, M.F., Zheng, J.P., 2013a. Constraints from zircon U-Pb ages, O and Hf isotopic compositions on the origin of Neoproterozoic peraluminous granitoids from the Jiangnan Fold Belt. South China. Contrib. Miner. Petrol. 166 (5), 1505–1519.
Zhao, J.H., Zhou, M.F., Zheng, J.P., Fang, S.M., 2010a. Neoproterozoic crustal growth and reworking of the Northwestern Yangtze Block: Constraints from the Xixiang dioritic intrusion. South China. Lithos 120 (3), 439–452.
Zhao, J.H., Zhou, M.F., Yan, D.P., Zheng, J.P., Li, J.W., 2011. Reappraisal of the ages of Neoproterozoic strata in South China: No connection with the Grenvillian orogeny. Geology 39 (4), 299–302.
Zhao, K.D., Jiang, S.Y., Sun, T., Chen, W.F., Ling, H.F., Chen, P.R., 2013b. Zircon U-Pb dating, trace element and Sr–Nd–Hf isotope geochemistry of Paleozoic granites in the Miao'ershan–Yuechengling batholith, South China: Implication for petrogenesis and tectonic–magmatic evolution. J. Asian Earth Sci. 74, 244–264.
Zhao, T.Y., Feng, Q.L., Metcalfe, I., Milan, L.A., Liu, G.C., Zhang, Z.B., 2017. Detrital zircon U-Pb-Hf isotopes and provenance of Late Neoproterozoic and Early Paleozoic sediments of the Simao and Baoshan blocks, SW China: Implications for Proto-Tethys and Paleo-Tethys evolution and Gondwana reconstruction. Gondwana Res. 51, 193–208.
Zhao, X.F., Zhou, M.F., Li, J.W., Wu, F.Y., 2008b. Association of Neoproterozoic A- and I-type granites in South China: Implications for generation of A-type granites in a subduction-related environment. Chem. Geol. 257 (1), 1–15.
Zhao, X.F., Zhou, M.F., Li, J.W., Sun, M., Gao, J.F., Sun, W.H., Yang, J.H., 2010b. Late Paleoproterozoic to early Mesoproterozoic Dongchuan Group in Yunnan, SW China: Implications for tectonic evolution of the Yangtze Block. Precambr. Res. 182 (1–2), 57–69.
Zheng, J.P., Griffin, W.L., O'Reilly, S.Y., Zhang, M., Pearson, N., Pan, Y.M., 2006. Widespread Archean basement beneath the Yangtze craton. Geology 34 (6), 417–420.
Zheng, Y.F., Zhang, S.B., Zhao, Z.F., Wu, Y.B., Li, X., Li, Z., Wu, F.Y., 2007. Contrasting zircon Hf and O isotopes in the two episodes of Neoproterozoic granitoids in South China: Implications for growth and reworking of continental crust. Lithos 96 (1–2), 127–150.
Zheng, Y.M., Shen, Q.X., Du, Q.L., Yuan, B.C., Ba, G.J., Zhang, N.D., Wang, Z.S., 1984. The geological report of the People's Republic of China, Derong Regional (scale 1: 200,000). Bureau of Geology and Mineral Resources of Sichuan Province, Sichuan, pp. 1-77. (In Chinese).
Zhou, M.F., Yan, D.P., Kennedy, A.K., Li, Y., Ding, J., 2002. SHRIMP U-Pb zircon geochronological and geochemical evidence for Neoproterozoic arc-magmatism along the western margin of the Yangtze Block. South China. Earth Planet. Sci. Lett. 196 (1–2), 51–67.
Zhou, M.F., Yan, D.P., Wang, C.L., Qi, L., Kennedy, A., 2006. Subduction-related origin of the 750 Ma Xuelongbao adakitic complex (Sichuan Province, China): Implications for the tectonic setting of the giant Neoproterozoic magmatic event in South China. Earth Planet. Sci. Lett. 248 (1–2), 286–300.
Zhou, X.Y., Yu, J.H., O'Reilly, S.Y., Griffin, W.L., Sun, T., Wang, X., Tran, M., Nguyen, D., 2018. Component variation in the late Neoproterozoic to Cambrian sedimentary rocks of SW China – NE Vietnam, and its tectonic significance. Precambr. Res. 308, 92–110.
Zhu, D.C., Zhao, Z.D., Niu, Y., Dilek, Y., Mo, X.X., 2011a. Lhasa terrane in southern Tibet came from Australia. Geology 39 (8), 727–730.
Zhu, D.C., Zhao, Z.D., Niu, Y.L., Dilek, Y., Hou, Z.Q., Mo, X.X., 2013. The origin and pre-Cenozoic evolution of the Tibetan Plateau. Gondwana Res. 23 (4), 1429–1454.
Zhu, G.L., Yu, J.H., Shen, L.W., Zhou, X.Y., 2018. Detrital zircon components of Sinian-Cambrian sedimentary rocks in SE Yunnan: Constrain on the boundary between Yangtze and Cathaysia blocks. Geol. J. China Univ. 24 (5), 658–670 in Chinese with English abstract.
Zhu, J.J., Hu, R.Z., Bi, X.W., Zhong, H., Chen, H., 2011b. Zircon U-Pb ages, Hf–O isotopes and whole-rock Sr–Nd–Pb isotopic geochemistry of granitoids in the Jinshajiang suture zone, SW China: Constraints on petrogenesis and tectonic evolution of the Paleo-Tethys Ocean. Lithos 126 (3), 248–264.
Zhu, J.G., Du, Q.L., Li, S.P., Wei, Z.P., Zeng, Y.F., Liao, Y.A., Lin, S.J., Wang, Z.S., Zheng, Y.M., 1984. In: The geological report of the People's Republic of China, Litang, Daocheng, and Gongling Regional (scale 1: 200,000). (In Chinese), pp. 1–232.
Zhu, W.G., Zhong, H., Li, Z.X., Bai, Z.J., Yang, Y.J., 2016. SIMS zircon U-Pb ages, geochemistry and Nd–Hf isotopes of ca. 1.0 Ga mafic dykes and volcanic rocks in the Huili area, SW China: Origin and tectonic significance. Precambr. Res. 273, 67–89.
Zhu, Y., Lai, S.C., Qin, J.F., Zhu, R.Z., Zhang, F.Y., Zhang, Z.Z., Zhao, S.W., 2019a. Neoproterozoic peraluminous granites in the western margin of the Yangtze Block, South China: Implications for the reworking of mature continental crust. Precambr. Res. 105443.
Zi, J.W., Cawood, P.A., Fan, W.M., Tohver, E., Wang, Y.J., McCuaig, T.C., 2012a. Generation of Early Indosinian enriched mantle-derived granitoid pluton in the Sanjiang Orogen (SW China) in response to closure of the Paleo-Tethys. Lithos 140–141, 166–182.
Zi, J.W., Cawood, P.A., Fan, W.M., Wang, Y.J., Tohver, E., McCuaig, T.C., Peng, T.P., 2012b. Triassic collision in the Paleo-Tethys Ocean constrained by volcanic activity in SW China. Lithos 144–145, 145–160.

Further reading

Dong, X., Zhang, Z.M., Santosh, M., 2010. Zircon U-Pb chronology of the Nyingtri Group, southern Lhasa Terrane, Tibetan Plateau: Implications for Grenvillian and Pan-African provenance and Mesozoic-Cenozoic metamorphism. J. Geol. 118 (6), 677–690.
Fergusson, C.L., Henderson, R.A., Fanning, C.M., Withnall, I.W., 2007. Detrital zircon ages in Neoproterozoic to Ordovician siliciclastic rocks, northeastern Australia: Implications for the tectonic history of the East Gondwana continental margin. J. Geol. Soc. London. 164 (1), 215–225.
Goodge, J.W., Myrow, P., Phillips, D., Fanning, C.M., Williams, I.S., 2004a. Siliciclastic record of rapid denudation in response to convergent-margin orogenesis, Ross Orogen, Antarctica. In: Detrital thermochronology - Provenance analysis, exhumation, and landscape evolution of mountain belts. Geological Society of America, Colorado, United States, pp. 105–126.
Goodge, J.W., Williams, I.S., Myrow, P., 2004b. Provenance of Neoproterozoic and lower Paleozoic siliciclastic rocks of the central Ross orogen, Antarctica: Detrital record of rift-, passive-, and active-margin sedimentation. Geol. Soc. Am. Bull. 116 (9–10), 1253–1279.
Li, Z.X., Li, X.H., Kinny, P.D., Wang, J., Zhang, S., Zhou, H., 2003. Geochronology of Neoproterozoic syn-rift magmatism in the Yangtze Craton, South China and correlations with other continents: Evidence for a mantle superplume that broke up Rodinia. Precambr. Res. 122 (1), 85–109.
Wang, L.J., Griffin, W.L., Yu, J.H., O'Reilly, S.Y., 2013a. U-Pb and Lu–Hf isotopes in detrital zircon from Neoproterozoic sedimentary rocks in the northern Yangtze Block: Implications for Precambrian crustal evolution. Gondwana Res. 23 (4), 1261–1272.
Zhu, Y., Qin, J.F., Zhu, R.Z., Zhang, F.Y., Zhang, Z.Z., Gan, B.P., 2019b. Petrogenesis and geodynamic implications of Neoproterozoic gabbro-diorites, adakitic granites, and A-type granites in the southwestern margin of the Yangtze Block. South China. J. Asian Earth Sci. 103977.